The Role of Autophagy in DNA Damage Repair

Camilla Trugenberger
St Cross College
MSc by Research in Oncology

Supervisor: Prof. Kristijan Ramadan
Second Supervisor: Prof. Vincenzo D'Angiolella

Word Count: 11945
Number of Figures: 12

Declaration of Contribution

All the experiments shown in the Results section were performed by me in the Ramadan laboratory under the supervision of Dr. Pauline Lascaux, unless otherwise stated. I have actively participated in the experimental design of these experiments. Techniques performed and presented in the following thesis include isolation of proteins on nascent DNA, immunofluorescence and denaturing immunoprecipitation. Dr. Lascaux has taught me various experimental techniques and provided experimental guidance in the laboratory. Experiments mentioned in the Discussion section but not shown in the Results section were performed by Dr. Lascaux.

Table of Content

LIST OF FIGURES 4

INTRODUCTION 6

Cancer and DNA Damage 6
Mechanism of Action of Camptothecin 7
TEX264, Autophagy and Genome Stability 9
The Nuclear Envelope Dynamics 10

AIMS OF THIS STUDY 12

MATERIALS & METHODS 13

Reagents 13
Cell Culture 15
Cell Transfection 15
Immunoblotting – Western Blot 15
Immunofluorescence 15
Immunoprecipitation 16
iPOND (isolation of Proteins on Nascent DNA) 17

RESULTS 18

Nanomolar vs Micromolar Doses: A Different Type of Damage 18
Autophagy at the Replication Fork 19
The Nuclear Envelope 22
Lamin A/C Acetylation 23
The Receptor TEX264 is SUMOylated upon CPT Treatment 24
24
Generation of TEX264 Mutants 24

DISCUSSION 26

Nanomolar VS Micromolar Doses: A Different Type of Damage 26
Autophagy and Replication 27
Autophagy Degrades Aggregated Proteins 28
Lamin A/C as a Marker for the Nuclear Envelope Plasticity after CPT Treatment 29
Lamin A/C Acetylation as Marker of Nuclear Envelope Permeability 30
TEX264 is SUMOylated after CPT Treatment 31
TEX264 Mutants 32

FUTURE DIRECTIONS 33

CONCLUSIONS 34

MODEL 35

ACKNOWLEDGMENTS 35

REFERENCE LIST 36

List of Figures

Figure 1. AlphaFold Prediction of TEX264 Structure.

Figure 2. Schematic of the Nuclear Envelope.

Figure 3. iPOND Assay Design.

Figure 4. Nanomolar doses of CPT Cause Replication Stress.

Figure 5. Autophagy Proteins at the Replication Fork.

Figure 6. 50 nM CPT Induce the Formation of Aggregates.

Figure 7. Depletion of TOP1 to Confirm it is the Aggregated Protein.

Figure 8. Lamin A/C Behavior upon CPT Treatment.

Figure 9. Lamin A/C Acetylation after 50 nM CPT.

Figure 10. TEX264 is SUMOylated upon Treatment with 50 nM CPT.

Figure 11. Validation of TEX264-Mutant Stable Cell Lines.

Figure 12. Model of Autophagic Degradation of TOP1cc.

Abstract

Camptothecin (CPT) is a genotoxic agent widely used for the treatment of colorectal cancer. It acts by preventing the hydrolysis of the covalent bond between Topoisomerase-I (TOP1) and DNA. TOP1 is an enzyme that relieves the topological stress caused by the unwinding of the helix during replication. The prevention of its release from DNA creates TOP1 cleavage complexes (TOP1ccs): bulky adducts that block the progression of DNA polymerases. TOP1ccs are highly toxic for replicative cells and need to be repaired. Although the proteasome plays a role in the degradation of TOP1ccs, the studies describing this have been conducted with micromolar doses of CPT, unreachable in clinical settings. Nanomolar doses of CPT are considered as more clinically relevant. Therefore, the DNA damage they cause, and the repair pathways involved need to be investigated further. Recently, it has been shown that the TOP1ccs induced by nanomolar doses of CPT are partially processed by the complex consisting of the unfoldase p97, the protease SPRTN and TEX264. TEX264 is a transmembrane protein located at both the nuclear envelope and the endoplasmic reticulum (ER). Interestingly, TEX264 is a key player in selective autophagy of the ER. Autophagy is the recycling mechanism of the cell and is essential for general cellular homeostasis. Autophagy has a dichotomous role in cancer due to both its tumor-suppressor and tumor-promoting effects. In fact, the upregulation of autophagy for the survival of hypoxic or chemotherapeutically-targeted cancer cells is currently being studied. Consequently, we hypothesised a role for autophagy in the repair of nanomolar dose-induced TOP1ccs. Here, we show that micromolar doses of CPT elicit a different type of DNA damage compared to the more clinically-relevant nanomolar doses. Interestingly, isolation of proteins on nascent DNA (iPOND) has allowed us to observe the increased presence of numerous autophagy proteins at the replication fork. This technique allows to pulldown proteins in close proximity to the replication fork. Additionally, we study the autophagy-dependent clearance of proteotoxic aggregates formed upon nanomolar CPT treatment, proposing an explanation for the irrelevance of the proteasome in this context. Finally, the regulation of the autophagy receptor TEX264 is investigated with regards to a specific post-translational modification arising after CPT treatment. Taken together, these findings show that autophagy plays a key role in the repair of the DNA damage caused by clinically-relevant doses of CPT.

Introduction

Cancer and DNA Damage

Cancer is a multi-faceted genetic disease, characterised by uncontrolled cellular division. Initially, cancer-causing mutations arise in tumour suppressor genes and oncogenes: tumour suppressor genes restrict cell growth whereas oncogenes promote it (Lee and Muller, 2010). A wide variety of events occurs downstream of these mutations, which make cancer the complex and intricate disease that it is. Cancerous cells are in fact able to avoid immune destruction, enable replicative immortality, resist cell death, promote genomic instability and further mutation and activate invasion and metastasis among other things (Hanahan, 2022). Mutations can be generated both endogenously and exogenously. More specifically, exposure to UV radiation and long-term use of tobacco and alcohol can be carcinogenic (Basu, 2018). These carcinogens cause DNA damage, which can also occur as part of the life of the cell. DNA damage is defined as any modification on the DNA resulting in changes in its coding properties or altering normal transcription and replication (Lindahl, 1993). It comes in a variety forms including, replication stress, DNA-Protein Crosslinks (DPCs), double-strand breaks and single-strand gaps (Martin, 2008). Cells have evolved repair mechanisms to deal with DNA damage and avoid carcinogenesis. Non-Homologous End-Joining (NHEJ) is a highly error-prone pathway to repair double-strand breaks whereby the two ends of the break are simply rejoined together (Chang et al., 2017). Homologous Recombination, on the other hand, uses the sister chromatid as template to repair the double-strand break and is, thus, much less likely to generate errors (Li and Heyer, 2008). In fact, one of the main cancer-causing mutations known is a mutation in the BRCA1/BRCA2 genes, which are crucial proteins in the HR pathway (Prakash et al., 2015). In fact, BRCA1/BRCA2-defective cells are not able to repair double-strand breaks through HR and, therefore, accumulate genetic mutations making them more prone to develop cancer. The proteins in DPCs can either be proteins in close proximity of the DNA caused to covalently attach to it by exogenous sources, or enzymes that work on the DNA that do not promptly detach from the it as part of their catalytic activity (Zhang et al., 2020). The better understanding of DNA damage has led to its exploitation for cancer therapy itself. In fact, most chemotherapeutic agents currently used act by generating DNA damage. For example, Cisplatin, widely used for testicular and cervical cancer, acts by creating intra-strand and interstrand crosslinks, which are highly toxic DNA lesions for cells (Woods and Turchi, 2013). Hence, it is of paramount importance to fully understand the mechanism by which chemotherapeutic agents cause DNA damage and the mechanisms by which this damage is repaired. The lack of specificity of most chemotherapeutic agents and the important side effects they trigger are a huge issue in the clinic. A better understanding of the DNA lesions they cause and how these are repaired could lead to the design of better cancer-specific drugs. Additionally, chemoresistance is another important issue encountered in the clinic, for which the study of specific DNA damage repair pathways is essential.

Mechanism of Action of Camptothecin

DNA replication is the process by which the DNA is duplicated prior to cell division. Obstacles or issues that result in the hampering, disturbance or slowing of this process are referred to as replication stress and are a major source of genomic instability (Gaillard et al., 2015). During DNA replication, the DNA helicase unwinds the two strands of the double helix to allow for the progression of the polymerase and the rest of the replicative machinery (Burnham et al., 2019). As a result of this unwinding, positive supercoiling occurs ahead of the replication fork and negative supercoiling is generated behind the fork (Liu and Wang, 1987). TOP1 is one of the main enzymes that relieves this topological stress. TOP1 binds to the DNA and creates a single-strand nick that allows the DNA to unwind (Wang, 2002). More specifically, the Tyr273 oxide group from TOP1's active site reacts with the 3' phosphate end of a nucleotide by transesterification: this results in the formation of a covalent phosphotyrosine bond and the breakage of the DNA's phosphodiester bond (Wang, 2002). Under normal conditions, as part of the catalytic cycle of TOP1, the covalent bond between the DNA and the enzyme is reversed, allowing TOP1 to religate the nick created (Pommier et al., 2006). This relegation process, whereby the DNA fragment are re-joined, relies on the alignment of the DNA end 5'-hydroxyl-group with the tyrosine-DNA phosphodiester bond (Pommier et al., 2006). However, naturally occurring DNA lesions, such as abasic sites or base oxidation can result in the stabilisation of TOP1cc (Gmeiner, 2019), (Pommier et al., 2022). More precisely, it is possible that the reversal of the covalent bond between TOP1 and the DNA is prevented: this stabilises TOP1 cleavage complexes (TOP1cc). This creates a highly toxic type of DNA lesion, which is a DPC. TOP1cc are bulky adducts that prevent the replication machinery from travelling through the fork (Katyal et al., 2014). Hence, TOP1cc are highly toxic for replicative cells. This led to their exploitation for cancer therapy. CPT is an analog for the drug Irinotecan, which is widely used for the treatment of various cancers including colorectal cancer (Fujita et al., 2015). Topotecan, Irinotecan, Belotecan and Trastuzumab Deruxtecan are CPT analogs approved for the treatment of small-cell lung cancer, colorectal cancer, ovarian cancer and HER2-low breast cancer respectively. In most cases, a first proteolytic step is necessary for the repair of TOP1cc; this can be mediated by the proteasome system, SPRTN and FAM111A among others (Sun et al., 2020). SPRTN is a metalloprotease, which preferentially binds double-stranded DNA and whose activity is controlled by a negative feedback loop mediated by its autocleavage (Stingele et al., 2016). It is essential for the repair of DPCs during S phase, whereby it uses the DNA as a bridge to come in proximity to its substrate and perform its catalytic activity (Vaz et al., 2016). After the proteolytic step, a remnant piece of protein still persists on the DNA. There exist various pathways for remnant excision. One is mediated by Tyrosyl-DNA-phosphodiesterase (TDP1). In essence, TDP1 hydrolyses the bond between the tyrosine on TOP1 and the 3' end of DNA (Pommier et al., 2006).The prior denaturation or proteolysis of TOP1 is required for TDP1 to elicit its complete activity (Yang et al., 1996). After the TOP1 has been removed by TDP1, the nick in the DNA is repaired through base excision mediated by the XRCC1 complex (Pommier et al., 2006). Another pathway for TOP1cc repair, which does not require a prior proteolytic step, involves 3' endonucleases, such as MRE11/Rad50/NBS1 (MRN complex), XPF-ERCC1, CtIP and APE2 (Chowdhuri and Das, 2021).

MRE11 is sensitive to DPC-induced double-strand breaks (Weickert and Stingele, 2022). The MRN complex consists of two MRE11 nucleases, two RAD50 ATPases and two NBS1 regulatory factors (Weickert and Stingele, 2022). In essence, MRE11 scans the DNA until the protein adduct is detected by the RAD50 ring-like structure, inducing a conformational change of the ring-like structure that activates MRE11. MRE11 then cleaves away the crosslinked protein. The resulting DNA break is then subsequently repaired by HR or NHEJ (Weickert and Stingele, 2022). Recently, however, the SPRTN-dependent upstream proteolysis of TOP1cc was discovered to be associated with the ATPase p97, which plays an essential role in chromatin-associated degradation (Krastev et al., 2022) (Kilgas et al., 2021) (Ramadan et al., 2017), and its cofactor TEX264. TEX264 is a Gyrl-like protein that sits at the intersection between autophagy and DNA damage repair (Fielden et al., 2022) In fact, it has been shown that TEX264 is able to recognise both unmodified and SUMOylated TOP1 (Fielden et al., 2020). It then recruits the unfoldase p97 and the protease SPRTN to remove TOP1 from the DNA. Briefly, p97 unfolds TOP1 to prepare it for SPRTN-mediated cleaving. This pathway is important during replication fork progression and specific to nanomolar doses of CPT. In fact, TEX264 inactivation only sensitises cells to nanomolar doses of CPT, and not micromolar doses (Fielden et al., 2020). Various pathways compete in the repair of TOP1cc but it seems like the SPRTN and TEX264-dependent one is more specific for nanomolar dose-induced TOP1cc.

TEX264, Autophagy and Genome Stability

Interestingly, at the same time as my group was publishing about TEX264 and its role in TOP1cc repair (Fielden et al., 2020), two groups described TEX264 as a major receptor for autophagy. More specifically, Chino et al. have shown that TEX264 is a receptor for autophagic degradation of the ER (Chino et al., 2019). Additionally, An et al. have further explored the role of TEX264 as an ER-phagy receptor and have described how it induces autophagy to remodel the ER upon nutrient stress (An et al., 2019). TEX264 is an ER-resident transmembrane protein (Chino et al., 2019), that also localises to the nuclear envelope (Fielden et al., 2020). In fact, the outer nuclear membrane and the ER membrane are continuous (Watson, 1955). It has various binding regions, through which it binds its cofactors (Figure 1). These are: the LC3-Interacting Region (LIR), through which it binds LC3, the GYR, the SUMO-Interacting Motif (SIM), that mediates binding to SUMOylated proteins, a SHP, which allows the interaction with p97, a phospho-binding site, which facilitates the binding with LC3 and, finally, a leucine-rich region (LRR), which is its transmembrane domain. The GyrI-like domain found in TEX264 is what allows him to bind TOP1; this binding is promoted when TOP1 is SUMOylated (Fielden et al., 2022).

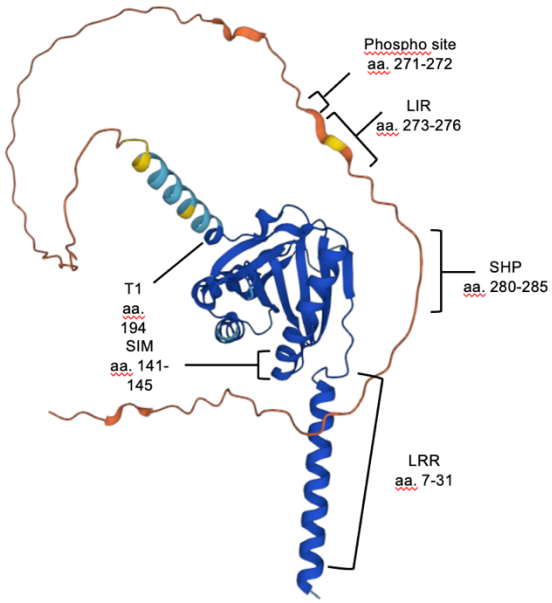


Figure 1. AlphaFold Prediction of TEX264 Structure. TEX264 is an ER and nuclear envelope-resident protein. It has a LIR, a SHP, a TBS, a SIM, a phospho-binding site and an LRR. These promote the binding with LC3, p97, TOP1 and SUMOylated proteins. The phosphor-binding site aids the binding to LC3-B and the LRR represents the transmembrane domain of TEX264.

Autophagy is the recycling mechanism of the cell, by which it breaks down misfolded protein or organelles into their constituent amino acids (Yu et al., 2018). The pathway is initiated by the activation of the ULK1 complex (ULK1, FAK, ATG13 and ATG101) (Shi et al., 2020), which, in turn, results in the activation of the Beclin 1-VPS34 complex, generating Phosphatidyl-inositol-3-phosphate (Agrotis and Ketteler, 2019). Several ubiquitin-like conjugation events occur on the ATG proteins for the formation of the phagophore. ATG7 is an E1 enzyme which acts with E2 enzyme ATG10 to form the ATG12-ATG5 complex. ATG7 also

activates LC3 (Nakatogawa, 2013). LC3, which exists in two forms, LC3-I and LC3-II, is recruited. LC3-I is unbound whereas LC3-II is lipidated and bound to the membrane of the phagophore, where it plays a role in its elongation (Satoo et al., 2009). LC3 is also essential for the selectivity of the autophagy protein (Johansen and Lamark, 2011). Selective autophagy is responsible for the degradation of specific, potentially detrimental cargo, such as aggregated proteins, damaged organelles or pathogens (Zaffagnini and Martens, 2016). Both bulk and selective autophagy rely on the formation of the phagophore, whose membrane elongates until it forms an autophagosome. The autophagosome fuses with the lysosome, whose highly acidic environment, rich in proteases, DNAses and lipases, will break down the proteins or organelles engulfed by the autophagosome into single amino acids, nucleotides or lipid structures (Yu et al., 2018).

Autophagy also plays a key role in genome stability. In fact, it has been extensively described that the autophagy pathway is upregulated upon treatment with various DNA-damaging agents, such as radiation or reactive oxygen species (Hewitt and Korolchuk, 2017). On the other hand, autophagy prevents the accumulation and progression of DNA damage by playing a key role in the senescence pathway (Ambrosio and Majello, 2020). Senescence is the irreversible exit from the cell cycle that occurs when the cell accumulates too much DNA damage to repair (Mylonas and O'Loghlen, 2022). Additionally, a recent study showed that autophagy is tightly linked with the adequate progression of the replication fork and that it is upregulated after replication stress-inducing agents (Vanzo et al., 2020). More precisely, autophagy is essential for the adequate control of the level of DNA damage checkpoint and repair proteins, as well as for the maintenance of a cellular energy level that allows for accurate DNA replication and repair (Holdgaard et al., 2019), (Karantza-Wadsworth et al., 2007).

As TEX264 is important for the repair of TOP1cc and is also a receptor for autophagy, we hypothesised that autophagy could play a role in the repair of nanomolar dose-induced TOP1cc. More specifically, we reasoned that the proteasome would degrade micromolar-induced TOP1cc from the DNA. On the other hand, TOP1cc caused by nanomolar doses of CPT could be degraded by autophagy, since the autophagy receptor TEX264 is essential for TOP1cc repair at nanomolar doses (Fielden et al., 2020)

The Nuclear Envelope Dynamics

The nuclear envelope surrounds the nucleus and separates it from the cytoplasm. It is composed of two lipid bilayers, the inner and the outer nuclear membranes and is continuous with the ER (Watson, 1955) (Figure 2). There are a wide variety of nuclear envelope-associated proteins that work to maintain the nuclear envelope stability and to regulate gene expression (Hetzer, 2010). Some of these proteins include Emerin, Lamins, Lamin-Associated Proteins 1 and 2 (LAP1/2), Lamin B Receptor (LBR) and nucleoporins.

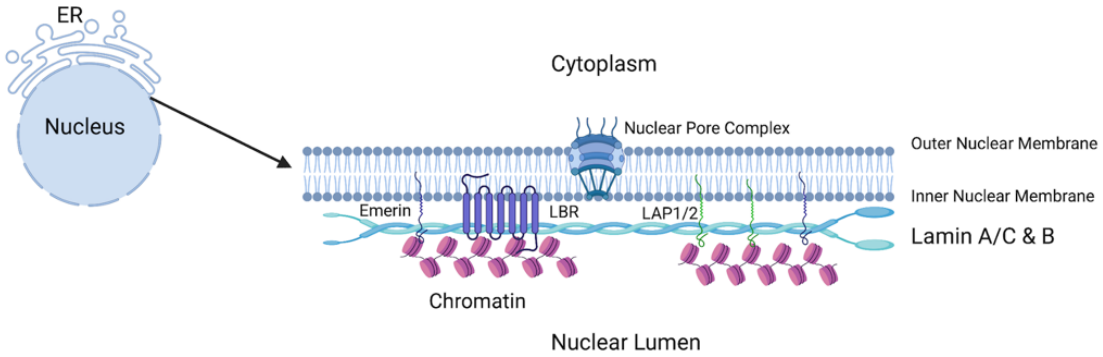


Figure 2. Schematic of the Nuclear Envelope. The inner and outer nuclear membranes consisting of two lipid bilayers form the nuclear envelope. This membrane encircles the nucleus and forms a continuum with the ER. There are various nuclear envelope-resident proteins that have roles from the maintenance of nuclear architecture and regulation of gene expression. Created with BioRender.

Emerin localises in the inner nuclear membrane and plays an important role in the maintenance of nuclear architecture (Koch and Holaska, 2014). The nuclear lamina is a meshwork of type V intermediate filaments composed of Lamin A, C and B (Karoutas and Akhtar, 2021). Lamins are an essential component of the nuclear envelope and act to maintain nuclear stability as well as chromatin function (Hetzer, 2010). They are regulated by post-translational modifications, such as phosphorylation, SUMOylation, methylation and acetylation. Phosphorylation of Lamin A/C mediates its depolymerisation for nuclear envelope breakdown. SUMOylation of Lamin A/C by UBC9 is involved in LC3-mediated nucleophagy. Furthermore, Lamin A/C methylation is thought to play a role in myoblast fusion (Karoutas and Akhtar, 2021). Finally, acetylation of Lamin A/C is important for the maintenance of nuclear architecture and modulates the permeability of the nuclear envelope (Karoutas et al., 2019).

Abnormalities in the nuclear lamina are associated with many diseases including cancer, premature aging, lipodystrophy, Werner Syndrome and Gerodermia osteodysplastica (Pande and Ghosh, 2023). Dysregulation of Lamin A/C protein level can have cancer-promoting effects. Low Lamin A/C levels promote malignancy by favoring genomic instability. On the other hand, elevated levels of Lamin A/C can have protective properties in response to mechanical stress in the context of cell migration (Karoutas and Akhtar, 2021).

Mechanical stress generated by chromosome relaxation/compaction dynamics can activate the ATR pathway, which in turn modulates the nuclear envelope plasticity (Kumar et al., 2014). Genomic instability is one of the hallmarks of cancer and it can be monitored by observing abnormalities in nuclear envelope morphology. More precisely, it has been described that the nuclear envelope can form blebs or micronuclei. These alterations of the nuclear envelope can be resolved by their fusion with the lysosome and the subsequent degradation of nuclear content (Bo Otto and Thumm, 2020).

All in all, the nuclear envelope is a highly dynamic membrane which is highly sensitive to DNA damage and remodels accordingly.

Aims of this Study

TEX264 has recently emerged as an important factor for both the repair of TOP1cc and ER-phagy (Fielden et al., 2020) (Chino et al., 2019). Thus, our group has proposed the concept that TEX264 is at the intersection between TOP1cc repair and autophagy (Fielden et al., 2022). More specifically, we hypothesise that TEX264 is the receptor for autophagic degradation of TOP1cc during DNA synthesis. To better understand this concept, I asked the following questions:

1. Whether autophagy proteins are present at stalled replication forks
2. If nanomolar and micromolar doses of CPT elicit different types of DNA damage
3. Why autophagy is necessary for the degradation of nanomolar dose-induced TOP1cc
4. Whether the receptor TEX264 is modified upon CPT treatment
5. If the nuclear envelope undergoes modifications after treatment with CPT

Materials & Methods

Reagents

- **Cell lines**

Cell line	Company/ Description
HeLa	ATCC/ Cervical cancer
HeLa TEX264 -/-*	Knock out of TEX264 protein
HeLa T1**	TEX264 was reintroduced in TEX264 -/- line with a mutation (E194A) in its TOPI-binding site and a V5 tag
HeLa LIR***	TEX264 was reintroduced in TEX264 -/- line with a mutation (F273A) in its LC3-interacting region and a V5 tag
HeLa SHP**	TEX264 was reintroduced in TEX264 -/- line with a mutation (G280R, G282R, L284A) in its p97-binding site and a V5 tag
HeLa WT**	TEX264 was reintroduced in TEX264 -/- and a V5 tag
HeLa Lamin GFP****	HeLa with GFP tag on Lamin A/C
HEK293	ATCC/ Human Embryonic Kidney

*These cells were generated by John Fielden (Fielden et al., 2020). Briefly, CRISPR/Cas9 knock-out of TEX264 were generated with 2.5μg of plasmids containing a guide RNA against TEX264 (sc-417333) and a puromycin resistance cassette (sc-417333-HDR). The cells were transfected with Fugene (Promega) at an early passage. After 72 hours, DMEM supplemented with puromycin was added to the cells for selection. After cell sorting into single-cell colonies, TEX264 levels were analysed with standard immunoblotting.

**For all the mutant cell lines, the pLX313-TP53-WT plasmid (RRID:Addgene_118014) was used as a backbone, which was modified to remove the TP53 sequence. The different TEX264 sequences were ligated into the backbone with the NEBuilder HiFi DNA Assembly Cloning Kit (New England Biolabs, E5520S). These cell lines were generated by John Fielden (Fielden et al., 2020).

***The LIR* was a gift from Haruka Chino and Noboru Mizushima. The stable cell line was generated by Gwendoline Hoslett in the same way as explained above.

****This stable cell line was produced by Dr. Pauline Lascaux with a pCDH_blast_MCS_Nard_GFP-Lamin (Addgene:RRID 167340) plasmid. HeLa cells were transfected with Fugene (Promega). The blasticidin resistance cassette allowed for selection of successfully transfected clones.

- **Antibodies**

Antibody	Specie	Reference	Company
Lamin A/C	Mouse	4777T	Cell Signalling Technologies
LAMP1	Rabbit	9091T	Cell Signalling Technologies
53BP1	Rabbit	SC-22760	Santa Cruz Biotechnology
γH2AX	Mouse	05-636	Merck Millipore
Alexa Fluor anti-rabbit 488	Donkey	A21206	Invitrogen
Alex Fluor anti-mouse 555	Donkey	A31570	Invitrogen
SUMO1	Rabbit	ab11672	Abcam
Ubiquitin	Mouse	1510	Merck Millipore
Vinculin	Mouse	SC-73614	Santa Cruz Biotechnology
GAPDH	Mouse	MA5-1573	Invitrogen
α-Tubulin	Mouse	T6199	Sigma-Aldrich
TOP1	Rabbit	A302-589A	Fortis Life Sciences
p97	Rabbit	10736-1-AP	Proteintech
LC3-B	Rabbit	2775S	Cell Signalling Technologies
TEX264	Rabbit		Non-commercial
Beclin-1	Rabbit	11306-1-AP	Proteintech
PCNA	Mouse	ab29	Abcam
CHMP7	Rabbit	16424-1-AP	Proteintech
SNAP29	Rabbit	ab138500	Abcam
Histone H3	Rabbit	ab1791	Abcam
ATG7	Rabbit	8558S	Cell Signalling Technologies
pCHK1 S345	Rabbit	2348S	Cell Signalling Technologies
Pol-α	Rabbit	ab31777	Abcam
Acetylated-Lysine	Rabbit	9441	Cell Signalling Technologies

The dilution used for immunofluorescence was 1:500 and 1:1,000 for immunoblotting.

Cell Culture

All cells were grown in DMEM supplemented with 10% heat-inactivated FBS and 1x Penicillin-Streptomycin at 37°C and 5% CO_2. Trypsin was used for splitting and was quenched with fresh DMEM. Regular mycoplasma testing was conducted using the MycoAlert Mycoplasma detection kit (Lonza).

Cell Transfection

For transient transfection, cells were seeded in 15cm dishes and grown overnight. 8ml of DMEM without supplements were added to the dishes. Plasmids were added to 500μL of Optimem at 37°C as was Fugene (Promega) or PEI. The plasmids and Fugene or Pei were mixed together and left at 37°C for 15'. These were then added onto the cells. The media was changed to supplemented DMEM between 6 and 16 hours after transfection.

Immunoblotting – Western Blot

Cells intended for standard immunoblotting were seeded in 6cm dishes for 48 hours. The plates were manually scraped and the collected cells were washed twice in 1x PBS. Lysis was done using complete RIPA buffer containing protease and phosphatase inhibitors as well as NEM. Seven cycles of 30'' ON 30'' OFF sonication followed. Lysates were spun at 21380g for 15', after which the supernatant was collected and used for protein quantification with the Bio-Rad BCA kit. The normalised volumes of lysates were supplemented with mQ water and 5x Laemmli Buffer and boiled at 95°C for 5'. The samples were subsequently loaded onto 5%-18% homemade acrylamide gels. Tris-Glycine running buffer was used for electrophoresis at 120V. The acrylamide gels were transferred onto PVDF or nitrocellulose membranes, depending on antibody, using Tris-Glycine transfer buffer and electrophoresis at 100V for 1 hour 15'. Membranes were incubated in 5% milk in 1xTBS containing 0.1% Tween (TBS-T) for 1 hour to avoid unspecific binding. After three washes with TBS-T, membranes were incubated in 5% BSA in TBS-T with 0.02% NaN_3 containing the appropriate volume of primary antibody overnight at 4°C. Three further washes with TBS-T preceded the incubation in secondary antibody in 5% milk in TBS-T at the appropriate concentration for at least 1 hour at room temperature. Pierce ECL Chemiluminescent Substrate (Pico or Femto, ThermoFisher) was used to detect the proteins on the iBright Imaging System (ThermoFisher).

Immunofluorescence

Cells were seeded in 96 well-plates at approximately 30% confluence. All solutions hereafter were added at 100μL/well. For CPT treatment, cells were treated with the appropriate concentration of CPT diluted in DMEM prior to collection. Cells were fixed with 4% Formaldehyde for 15' at 4°C and permeabilised with 0.5% Triton for 15' at room temperature. Unspecific binding was avoided by blocking at 37°C for 1 hour with 5% BSA in 1x PBS. Primary antibodies were diluted in 2.5% BSA diluted in PBS for 1 hour at room

temperature and added to each well. Secondary antibodies and DAPI were added in identical manner. The cells were washed twice with 1x PBS and 100μL of 1x PBS were left in each well. The plate was sealed with an airtight translucent film and covered in foil; it was in turn kept at 4°C. Images were taken with the Zeiss-710 confocal microscope. Only one stack was taken per image. Image analysis was conducted with Fiji (ImageJ) and CellProfiler. Prism 9 (GraphPad) was used for statistical testing.

For the detection of aggregated proteins, the protocol was adapted to avoid high background staining due to the high affinity of the Proteostat dye to the plastic of the plate. Cells were seeded on glass cover slips in 6 well-plates at approximately 40% confluence. Blocking of unspecific binding was done in 5% BSA in 1x PBS with 3mM EDTA to avoid staining of lipid membranes. Proteostat staining was used at a concentration of 1:2000 and washed 5 times with PBS containing 0.1% BSA, 0.2% Tween and 0.3mM EDTA, then washed twice with 2x PBS. After incubation with secondary antibodies and DAPI, coverslips were dipped 3 times in mQ water and mounted onto slides with Fluoromount G (ThermoFisher).

Immunoprecipitation

Lysis Buffer: 50mM Tris HCl (pH 7.4), 150mM NaCl, 1mM EDTA, 0.5%Triton
Benzonase Buffer: 50mM Tris HCl (pH 7.4), 150mM NaCl, 2mM $MgCl_2$
Beads Buffer: 50mM Tris HCl (pH 7.4), 150mM NaCl
Denaturing Wash Buffer: 50mM Tris HCl (pH 7.4), 1M NaCl, 1% Triton
Wash Buffer: 50mM Tris HCl (pH 7.4), 0.1% Triton, 0.1M NaCl

Cells were seeded in 15cm dishes at least 24 hours before collection by manual scraping. For CPT treatment, cells were treated with the appropriate concentration of CPT diluted in DMEM prior to scraping. The collected cells were washed twice with 1x PBS before being resuspended in lysis buffer and rotated at 4°C for 20'. Centrifugation for 5' at 1,000g followed. Benzonase buffer was used to wash the pellet once. Benzonase-Nuclease was added to benzonase buffer at a concentration of 1:1000. To digest the chromatin, cells were rotated in benzonase buffer containing benzonase nuclease for at least 1 hour at 4°C. Cells were centrifuged at 21380g for 15' and 20μL/sample were taken as input. V5-Trap Agarose beads (Proteintech) were washed twice with beads buffer. The pooled supernatant was incubated in 1.5 mL LoBinding Tubes (Eppendorf) with the washed beads for at least 2 hours by rotating at 4°C. 5μL of Ethidium Bromide were added to each tube. The beads were washed four times with denaturing wash buffer (to remove all proteins which were not covalently attached to the bait, used for detection of post-translational modifications) or with wash buffer (to maintain complexes, used for co-immunoprecipitation). Beads were eluted in 2x Laemmli Buffer (at least twice the volume of beads). Both input and elution were boiled at 95°C for 10'. The samples were then loaded onto acrylamide gels used for immunoblotting.

iPOND (isolation of Proteins on Nascent DNA)

Click Reaction Cocktail: 10μM Biotin Azide, 10mM Sodium L-Ascorbate, 2mM $CuSO_4$

NTN Buffer: 100mM NaCl, 20mM Tris HCl (pH 7.4), 0.05% IGEPAL

The iPOND protocol was adapted from Sirbu et al. (Sirbu et al., 2012) and the experimental design from Nakamura et al. (Nakamura et al., 2021) (Figure 3). Briefly, HEK293 cells were seeded in 24.5cm trays and synchronised with 2mM thymidine for 17 hours. The cells were then released into S phase for three hours by washing the thymidine with fresh DMEM. Cells were labelled with 10mM EdU for 15' or treated with CPT for 20' and then labelled with EdU for 20' in the presence of CPT. Cells were fixed with 1% formaldehyde for 20', which was subsequently quenched with 0.125M Glycine. Three washes with 1x PBS followed. Cells were then permeabilised with 0.25% Triton and washed three times with 1x PBS. Next, cells were incubated in the click reaction cocktail for one hour at room temperature. DMSO was used in place of Biotin Azide for the negative control (no click). Lysis with 1% SDS containing phosphatase and protease inhibitors followed during 3 hours of 30'' ON 30'' OFF of sonication. 150μL of Pierce Streptavidin Beads (ThermoFisher Scientific) were washed twice with 1x PBS. Lysates were centrifuged at 16100g for 20' and the supernatant diluted with 1x PBS 1:1. 100μL were taken as input and mixed with 25μL 5x Laemmli buffer. The diluted supernatant was then added onto the beads and rotated at 4°C fort at least 16 hours. The supernatant was disposed of, and the beads washed with 1% SDS. The beads were subsequently washed once with 1M NaCl and twice with NTN buffer. Elution with 100μL of 2x Laemmli buffer and boiling at 95°C for 25' to reverse crosslinking followed. The input was boiled at 95°C for 10' only. The samples were then processed as per standard immunoblotting.

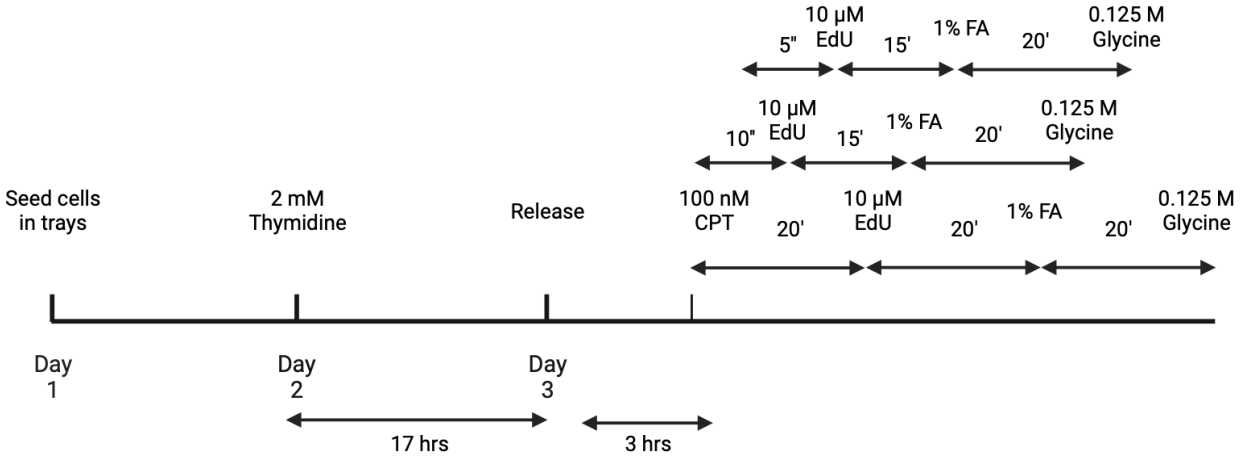


Figure 3. iPOND Assay Design. Three samples (negative control, untreated and CPT-treated) were processed separately. For CPT treatment, 100 nM CPT were added onto cells for 20', then added for further 20' with 10mM EdU. Otherwise, 10mM EdU were added to the cells for 15'. DNA-protein crosslinking with 1% Formaldehyde followed straight after for 20'. Finally, 0.125M Glycine was used to quench the Formaldehyde.

Results

Nanomolar vs Micromolar Doses: A Different Type of Damage

A study by Ray Chaudhuri and colleagues showed that different doses of CPT resulted in different types of DNA damage (Ray Chaudhuri et al., 2012). More precisely, these authors performed fiber assays in which they showed that 25nM CPT induced the net slowing of replication forks independently of double strand breaks, whereas 1μM CPT induced double strand breaks. The proteasome has long been thought of as the canonical TOP1cc degradation route. However, the studies describing this are usually conducted with micromolar doses of CPT (Desai et al., 2001), not nanomolar doses of CPT, which are thought to be more clinically relevant (Takimoto and Arbuck, 1997), (Slichenmyer et al., 1993). We reasoned that different doses of CPT would result in different types of DNA damage that would need to be resolved and degraded by two separate pathways. We first aimed to confirm Ray Chaudhuri et al.'s findings by performing an immunofluorescence assay with γH2AX and 53BP1 (Figure 4).

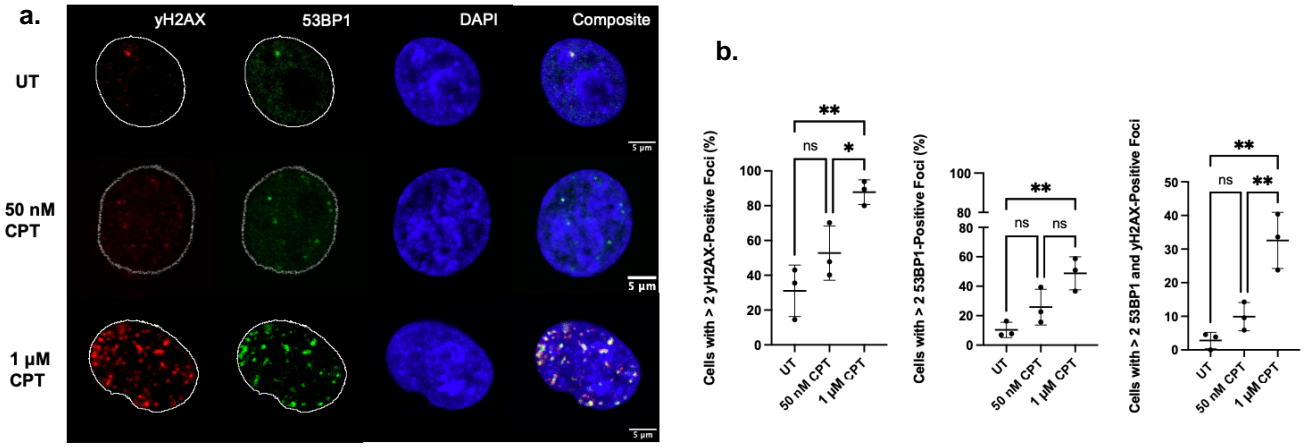


Figure 4. Nanomolar Doses of CPT Cause Replication Stress. **a** Immunofluorescence was used to detect γH2AX and 53BP1 foci after treatment with 50 nM CPT or 1μM CPT for 1 hour. **b** Both 53BP1 and γH2AX foci, as well as double-positive foci, were counted with a specific CellProfiler pipeline. Statistic al significance was determined with a one-way ANOVA. Cells treated with 50 nM CPT showed less double-positive foci compared to those treated with 1μM CPT. The fewer number of double-positive foci indicates that the DNA damage caused is likely to be replication stress instead of double-strand breaks, marked by double-positive foci. n=3, *: p< 0.05, **: p< 0.01.

γH2AX is an overall marker of DNA damage. In fact, it is one of the first signaling events to occur upon DNA damage and is, therefore, a marker of general DNA damage (Gagou et al., 2010). On the other hand, 53BP1 is involved in NHEJ and is, thus, a more specific marker for double strand breaks (Gupta et al., 2014). Foci positive for both γH2AX and 53BP1 would be sites of double-strand breaks; whereas foci only positive for γH2AX would hint more towards replication stress, although this requires further confirmation. We used this assay to discriminate between these two different types of DNA damage. Cells treated with 50 nM CPT had seemingly more γH2AX-positive foci and less double-positive foci compared to cells treated with 1μM CPT. This suggest that nanomolar doses of CPT are more likely to cause replication stress compared to the micromolar doses, more likely to induce double-strand breaks, which is consistent with Ray Chaudhuri et al.'s findings. It is, however, important to note that some colocalization still ocurrs in 50 nM CPT-treated cells. Hence, the formation of double-strand breaks at this dose is not excluded.

Autophagy at the Replication Fork

Since we confirmed that nanomolar and micromolar doses of CPT elicit different types of DNA damage, we focused on nanomolar doses of CPT, which we hypothesised were associated with autophagy. To investigate whether treatment with 100 nM CPT, which is 10-fold lower than doses used in other similar studies (Nakamura et al., 2021), would enhance the recruitment of autophagy proteins at the stalled replication fork, we performed an iPOND assay (Figure 5). This technique allows the purification of proteins in close proximity to newly synthesised DNA labelled with EdU.

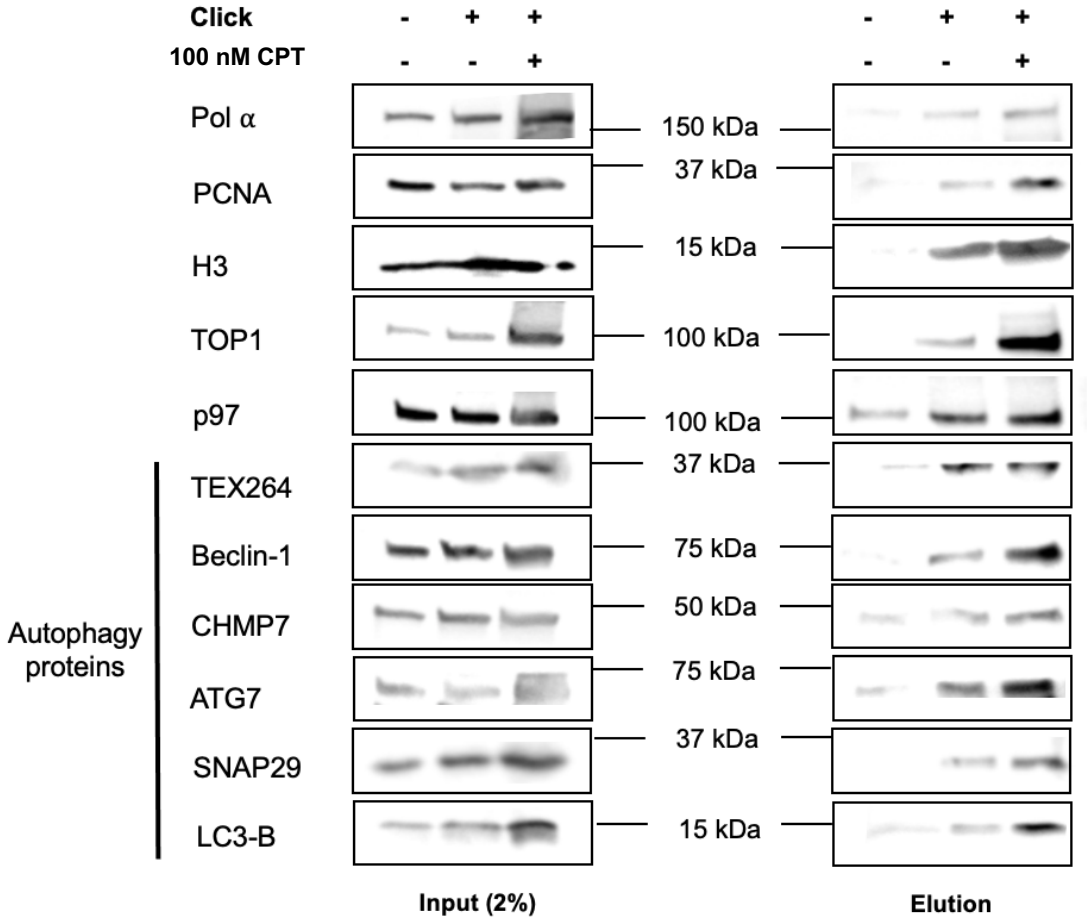


Figure 5. Autophagy Proteins at the Replication Fork. An iPOND assay was performed to isolate proteins in close proximity to the replication fork (elution). The input represents the whole cell extract. Biotin azide was replaced with DMSO in the negative control (no click) to prevent the click reaction from happening. Six key autophagy proteins are increased after 100 nM CPT treatment. n=2

In essence, the iPOND assay relies on the incorporation of EdU by replicating cells. All components in close proximity and at the replication fork are crosslinked after incubation with Formaldehyde. Click chemistry is then performed to attach Biotin Aizde to the EdU incorporated into the DNA of the cells. Immunoprecipitation with Streptavidin beads, which bind the Biotin Azide allow for the pull-down of the replication fork an all proteins in close proximity to it (Dungrawala and Cortez, 2015). Polymerase α (Pol α), PCNA and Histone H3 were used as positive controls. Pol α acts together with the DNA primase at the origin of replication as

well as for the synthesis of Okazaki fragments (Muzi-Falconi et al., 2003). PCNA sits around the DNA and is essential to ensure processive DNA synthesis (Kelman, 1997). Histone H3 is one of the main histones, proteins whose role is to pack the DNA. Next, we looked at TOP1 and p97, which both showed an increase upon CPT treatment, as expected. We then observed that the autophagy receptor TEX264 was also present at the replication fork. Interestingly, we noticed the presence five key autophagy proteins at the stalled replication fork after 100 nM CPT treatment. Beclin-1 and VPS34 are important for the initiation and regulation of the autophagy pathway and play a key role in directing the pre-autophagosome to the cargo proteins (Kang et al., 2011). CHMP7 is part of the ESCRT-III complex and participates in phagophore closure (Takahashi et al., 2018). Another important protein we wanted to study is ATG7, which is essential for the lipidation of the ubiquitin-like protein LC3. SNAP29 is part of the SNARE protein family, whose role in membrane fusion is essential for processes such as the fusion between autophagosome and lysosome (Tian et al., 2021), the final step of the autophagy pathway. Finally, we were interested in LC3-B, which is essential for selective autophagy as well as for the elongation of the phagophore (Lee and Lee, 2016). It is important to note that there is an overall increase of proteins in the click + 100 nM CPT condition in the input overall. Although it seems like the autophagy proteins are enriched at the replication fork after treatment with 100 nM CPT, it is difficult to uncouple this from the overall increase of proteins in this condition in the input overall.

Autophagy Removes Aggregated TOP1cc

Next, we asked if autophagy could play a role in the degradation of nanomolar dose-induced TOP1cc. It is known that one of the main roles of autophagy is to remove misfolded organelles and proteins, which tend to form aggregates (Das et al., 2012). As the proteasome usually degrades small and soluble cargo, bulky insoluble aggregates are better dealt with by the autophagy machinery than by the proteasome (Lamark and Johansen, 2012). Hence, we proposed that inhibition of autophagy could facilitate the visualisation of aggregated proteins induced by nanomolar doses of CPT. To investigate this, we used a dye optimised for immunofluorescence that specifically fluoresces when embedded in the tightly bound beta-sheaths of aggregated proteins (Bagnoli et al., 2023) (Figure 6).

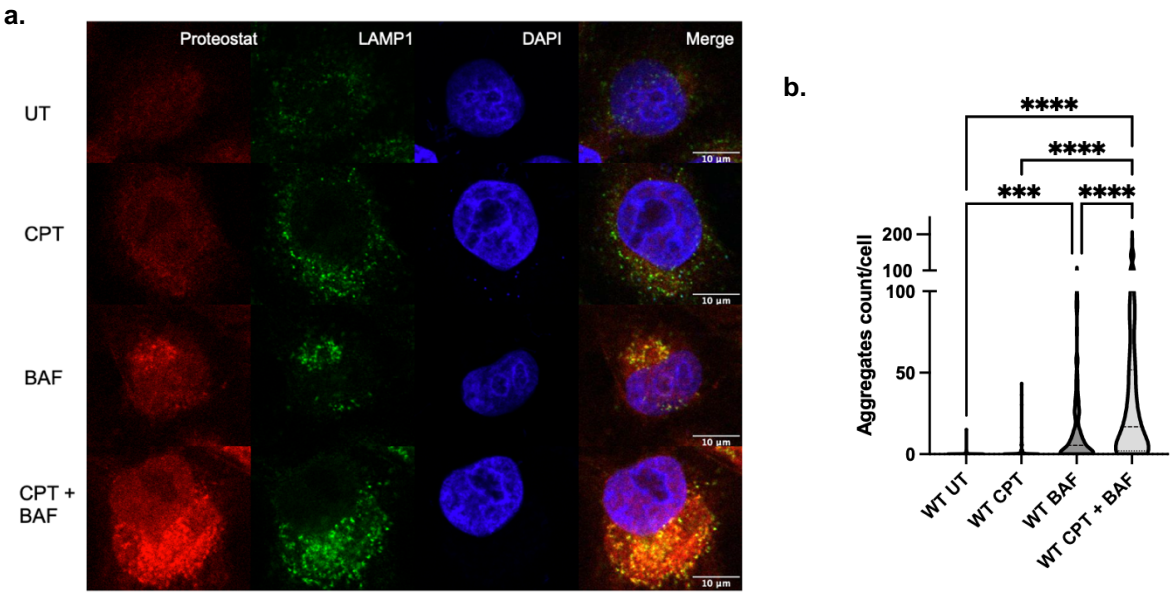


Figure 6. 5 0nM CPT Induces the Formation of Aggregates. **a** Immunofluorescent staining of aggregated proteins (Proteostat) and lysosomes (LAMP1). 50 nM Bafilomycin were used to block the acidification of lysosomes. **b** CellProfiler was used to quantify the number of aggregates per cell. 50 nM Bafilomycin induced a higher level of aggregated proteins compared to untreated of 50 nM CPT-treated cells. However, cells treated with both 50 nM CPT and 50 nM Bafilomycin showed an even greater number of aggregated proteins per cell. n=3, two-way ANOVA ***: p< 0.001, ****: p< 0.0001

50 nM Bafilomycin was used to inhibit the acidification of the lysosome, preventing the degradation of the autophagy cargo proteins. This was done to prevent the degradation of potentially aggregated TOP1cc making them visible by immunofluorescence. LAMP1, a marker for late endosomes and lysosomes was used in conjunction with the Proteostat dye. Autophagy inhibition with 50 nM Bafilomycin resulted in an increase in aggregated proteins, which was even higher when 50 nM Bafilomycin were given together with 50 nM CPT. Autophagy is crucial for the clearance of aggregated proteins formed upon treatment with 50 nM CPT.

To confirm that the aggregated proteins we observed were, in fact, TOP1cc, we sought to deplete TOP1 from the cells (Figure 7). Without TOP1, the increase we noted in the presence of both CPT and Bafilomycin should no longer be visible.

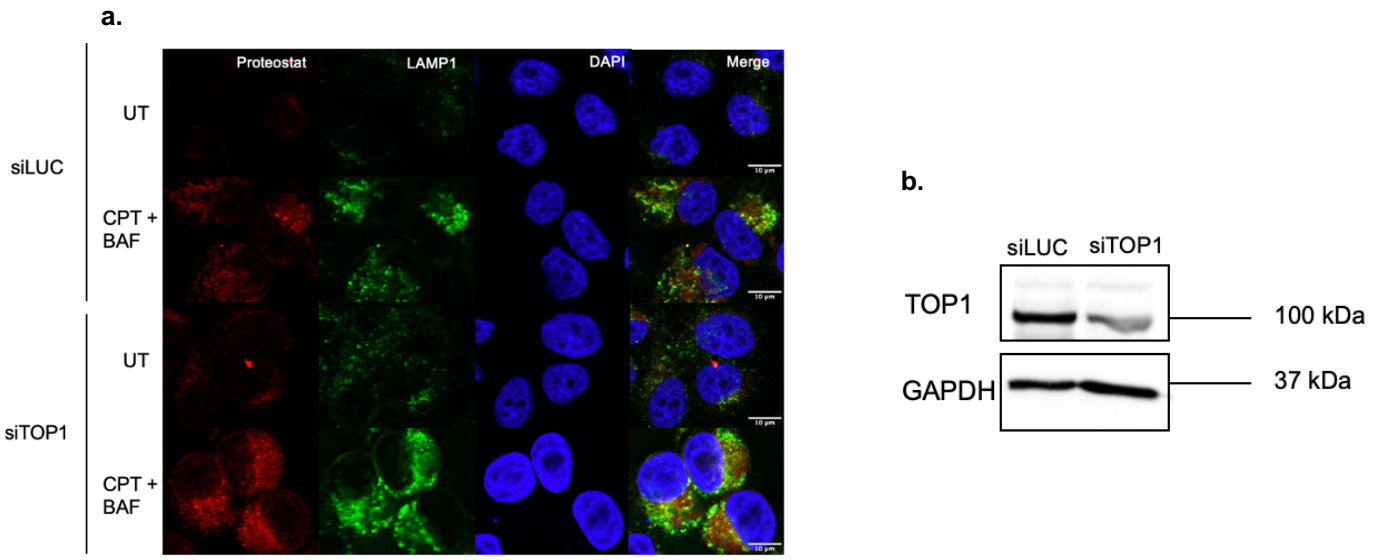


Figure 7. Depletion of TOP1 to Confirm it is the Aggregated Protein. **a** Immunofluorescent staining of aggregated proteins (Proteostat) and lysosomes (LAMP1) with siRNA against Luciferase and siRNA against TOP1. Cells were treated with 50 nM CPT and 50 nM Bafilomycin for at least 16 hours and at most 24 hours. **b** Western Blot analysis of TOP1 expression in cells treated with siLuciferase and siTOP1. GPADH was used as a loading control. n=3

However, the depletion level of TOP1 was not enough to draw any conclusions about this experiment. TOP1 -/- stable cell lines could be used instead to validate our conclusions.

The Nuclear Envelope

As autophagy is a cytosolic degradation pathway, the selected nuclear cargo would have to breach the nuclear envelope in order to be incorporated into the autophagosome. Therefore, we aimed to better study the nuclear envelope and its behavior upon CPT treatment. As a marker for the nuclear envelope we used Lamin A/C. Lamins A and C are type V intermediate filaments essential for the stiffness and integrity of the nuclear envelope (Lammerding et al., 2006), (Fisher et al., 1986). We used immunofluorescence to visualise lamin a/c as well as LAMP1 upon CPT treatment (Figure 8).

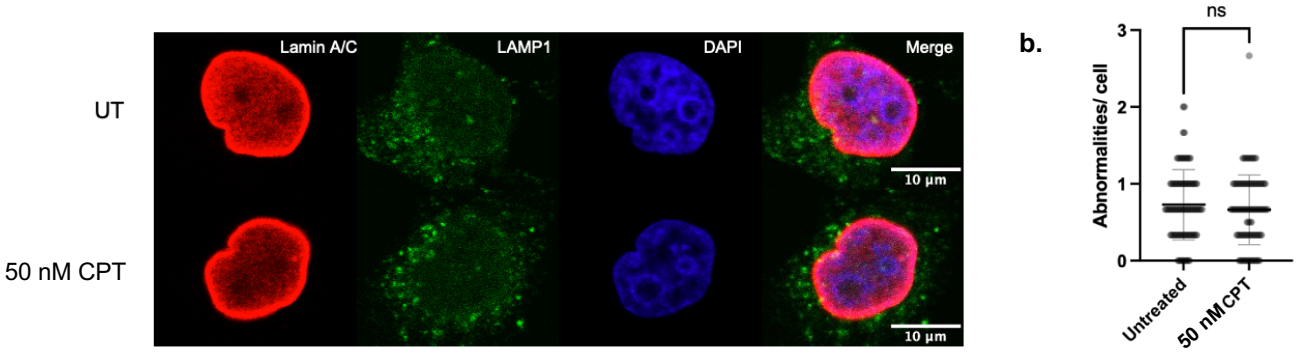


Figure 8. Lamin A/C Behavior upon CPT Treatment. **a.** Immunofluorescence of HeLa cells after 1 hour of 50 nM CPT treatment. **b.** Quantification of nuclear envelope abnormalities/ cell. Abnormalities were defined as invaginations, blebs or micronuclei and were counted manually. A non-parametric t-test was performed to determine statistical significance. n=3

We manually counted the abnormalities of the nuclear lamina per cell. These were defined as blebs, invaginations or micronuclei. No statistical significance was observed between untreated and 50 nM CPT-treated cells, indicating that Lamin A/C does not undergo significant morphological changes after treatment with CPT.

Lamin A/C Acetylation

As no changes in the shape of the nuclear envelope were observed, we asked whether CPT treatment could render the nuclear envelope more permeable. Karoutas et al. showed that changes in lamin acetylation levels can result in its increased solubility and transient nuclear envelope rupture (Karoutas et al., 2019). We hypothesised that CPT treatment could correlate with lamin deacetylation. We performed a denaturing immunoprecipitation over GFP-Lamin A/C to study acetylation levels (Figure 9).

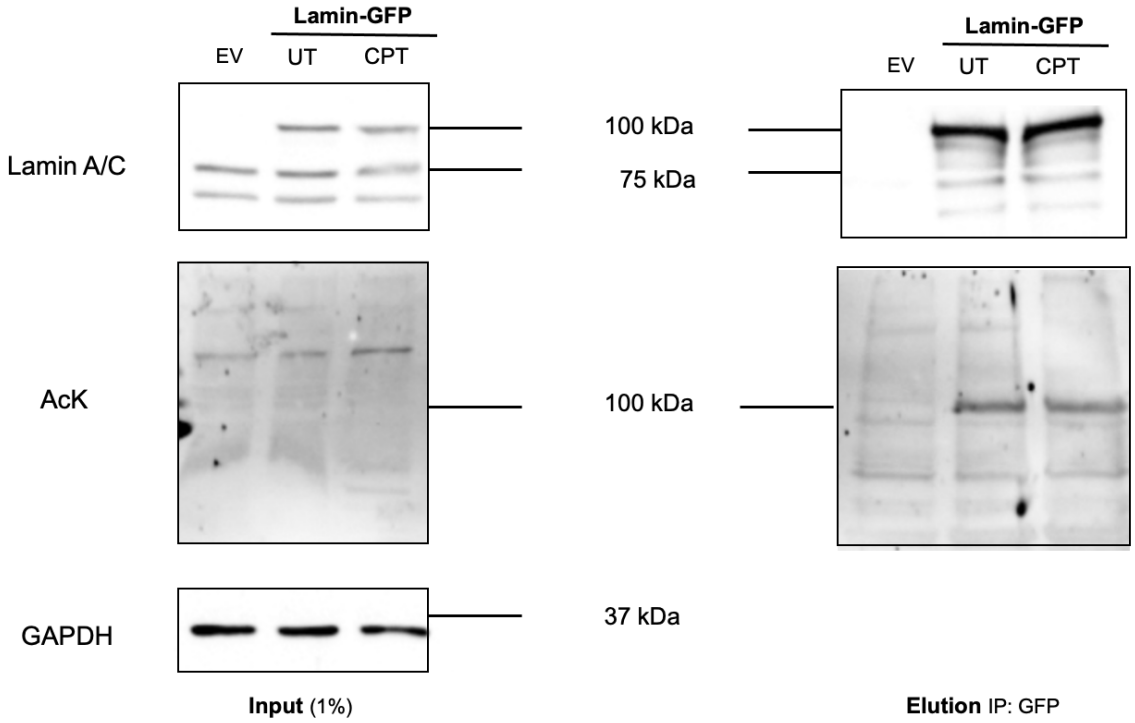


Figure 9. Lamin A/C Acetylation after 50 nM CPT. Denaturing immunoprecipitation over GFP tag on Lamin A/C of HeLa cells. Acetylation levels were measured with an antibody against acetylated lysines. 3 separate experiments were performed but variable results were observed.

We confirmed that Lamin A/C is acetylated using an antibody that recognises all acetylation events. Three biological repeats were performed and no significant changes in acetylation levels were noticed after CPT treatment.

The Receptor TEX264 is SUMOylated upon CPT Treatment

TEX264 has previously been described as the main receptor for ER-phagy (Chino et al., 2019) and as an essential factor for TOP1cc repair (Fielden et al., 2020). TEX264 is also present at the replication fork (Figure 3). Often, receptors undergo modifications that enable them to become activated or undergo conformational changes. We wondered whether TEX264 underwent any modifications upon treatment with CPT. We reasoned that TEX264 could be modified by some post-translational modifications. More specifically, we studied SUMOylation and ubiquitination (Figure 10).

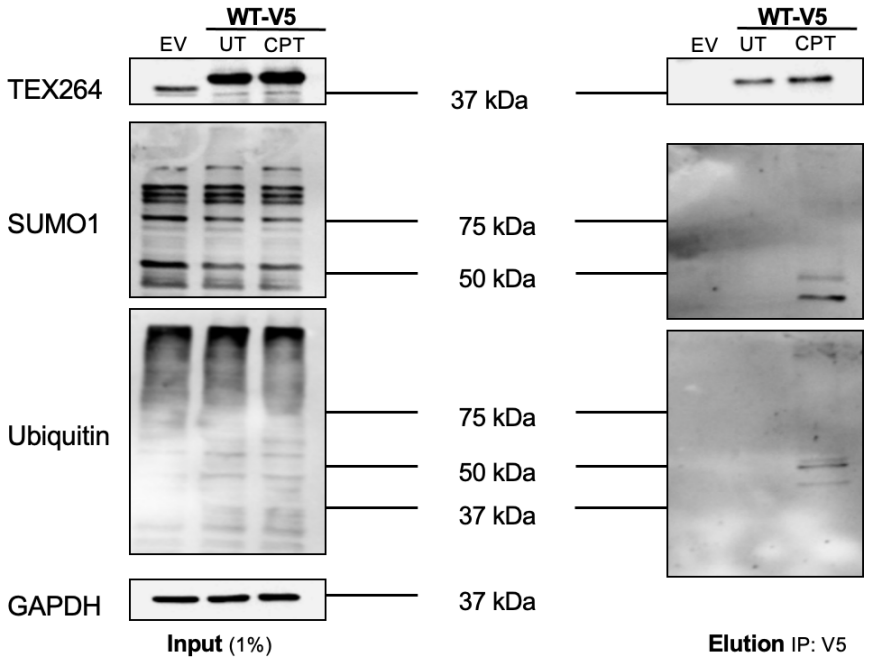


Figure 10. TEX264 is SUMOylated upon Treatment with 50 nm CPT. Denaturing immunoprecipitation over the V5 tag introduced in HeLa WT cells. HeLa cells were used for the empty vector. SUMO1 and ubiquitin levels of TEX264 were increased after treatment with 50 nM CPT for 1 hour. n=3 for SUMO1 and n=2 for ubiquitin

SUMO1 is a small ubiquitin-like modifier involved in a wide variety of cellular processes. These range from the response to DNA damage to the regulation of gene expression all the way to cell cycle progression (Vertegaal, 2022). Ubiquitin also has a broad panoply of roles within the cell. Apart from its widely described role in the targeting of proteins for proteasomal degradation, ubiquitin is also important in DNA damage repair, protein trafficking and cell proliferation among many others (Guo et al., 2023). We observed that both SUMOylation and ubiquitination levels of TEX264 were increased after treatment with 50 nM CPT.

Generation of TEX264 Mutants

In order to further study the role of TEX264 as an autophagy receptor, we generated stable cell lines displaying either wild type TEX264 or mutated TEX264. More specifically, we aimed to discern which of its domains were essential for TEX264's role as receptor for autophagic degradation of TOP1cc. To do this, we introduced mutations in its TOP1-binding site, LIR and SHP, which abolished its interaction with TOP1, LC3 and p97 respectively. We aimed to confirm that the mutations introduced did, in fact, lead to the loss

of the interactions mediated by each specific domain. To do this, we performed various co-immunoprecipitation assays to assess the interactions (Figure 11).

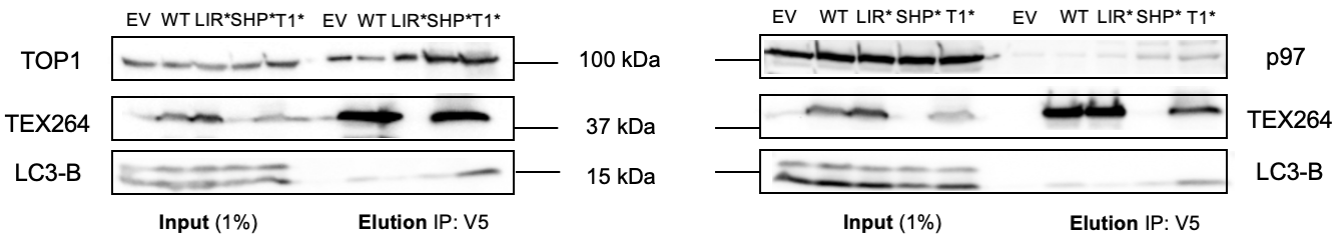


Figure 11. Validation of TEX264-Mutant Stable Cell Lines. Co-immunoprecipitation over the V5 tag present in stable cell lines.

Six separate experiments were performed; however, variable results were observed. Hence, no reliable conclusions regarding the stable cell lines could be made.

Discussion

Nanomolar VS Micromolar Doses: A Different Type of Damage

Our immunofluorescence assay allowed us to observe a difference in the type of DNA damage caused by different doses of CPT: nanomolar dose of CPT caused replication stress whereas micromolar doses resulted in double-strand breaks (Figure 4). This idea is further corroborated by a study from Huang and colleagues (Huang et al., 2010). Huang et al. performed immunoblotting assays on whole cell extracts of HCT116 cells after treatment with 100 nM and 1 μM CPT for 2 hours. In particular, they studied the phosphorylation of ATM and noticed a net increase upon treatment with 1μM CPT compared to the cells treated with 100 nM CPT. Generally, the ATM pathway is responsible for sensing and initiating the response to double-strand breaks whereas ATR senses replication stress and single-strand gaps (Awasthi et al., 2015). The significant increase in ATM phosphorylation upon treatment with 1μM CPT suggests that this dose of CPT causes double-strand breaks. TOP1 adducts can impede the progression causing a stalled fork. If this is not promptly resolved, lethal double-strand breaks can occur (Schoonen et al., 2019). It is expected that increasingly higher doses of CPT would tend to cause double-strand breaks. It is also worth noting that the incubation time of CPT could also influence what type of DNA damage we observe. It would be useful to repeat this experiment and monitor the formation of foci over time. Perhaps the longer the incubation time, the likelier DNA double-strand breaks can occur. However, other studies have observed the activation of the replication stress pathway upon treatment with 1 μM CPT (Ribeyre et al., 2016), (Xu et al., 2015). Additionally, Iannascoli and colleagues performed a COMET-assay with both nanomolar and micromolar doses and observed the occurrence of double-strand breaks only in the cells treated with micromolar doses (Iannascoli et al., 2015). COMET is a direct measure of DNA damage, whereas fibers, phosphorylated checkpoints and foci are an indirect measure. Finally, Chaudhuri et al. also performed a COMET assay as well as a BrdU incorporation assay in the presence of 25nM and 1 μM CPT (Ray Chaudhuri et al., 2012). They observed a decrease in fork progression and fork reversal uncoupled from double-strand breaks in the presence of 25 nM CPT. Synchronising cells to monitor the formation of γH2AX and 53BP1 foci during S phase and outside of S phase after 50 nM CPT could help discriminate between replication stress and double-strand breaks.

The fact that different doses of chemotherapy elicit different effects has also been described for doxorubicin. In fact, Park et al. have described that low dose and high-dose doxorubicin induce cell death through mitotic catastrophe and apoptosis respectively (Park et al., 2005). Huh-7 cells were treated with 10μg/ml or 50ng/ml of doxorubicin and then processed for TUNEL assay, used to detect DNA fragmentation associated with apoptosis. They observed much higher levels of DNA fragmentation in cells treated with 10μg/ml.

Autophagy and Replication

To explore the presence of autophagy proteins at the replication fork after treatment with CPT, we reproduced Nakamura et al.'s iPOND experimental design (Nakamura et al., 2021) (Figure 5). We were able to reproduce their results and observed an increase in PCNA levels at the replication fork after CPT. Treatment with CPT prevents the progression of replication. As a response, new origins are fired, increasing the number of forks pulled down and, thus, leading to the increased presence of PCNA. However, the dose of CPT used in their study was 1 μM CPT instead of 100 nM CPT. They observed an increase in TOP1 levels, as did we. This was expected as TOP1 is trapped onto the chromatin by CPT. Nakamura et al.'s proteomics study, as well as my group's previous work on TEX264 (Fielden et al., 2020), showed that TEX264 is present at the replication fork. They also used Roscovitine to inhibit new origin firing. After treatment with both CPT and Roscovitine, TEX264 levels are increased in the iPOND data. This suggests that TEX264 is not present at new origins, but mainly localised at stalled replication forks. We did not observe any change in TEX264 levels between untreated and CPT-treated cells, which is in line with their findings. Thus, TEX264 is present at stalled replication forks and newly fired origins mitigate its enrichment. In Nakamura et al.'s proteomics data there were also some autophagy proteins including ATG7, SNAP29 and CHMP7. All three of these proteins are increased at replication forks in their proteomics. As previously mentioned, we observed an increase in protein levels overall in the input of the click + 100 nM CPT condition, which could be responsible for the increase of proteins in the same condition of the elution. Additionally, it would be useful to repeat this experiment with the inhibition of the Cdc7 kinase, which promotes new origin firing in S phase (Bousset and Diffley, 1998) and is, thus, more specific than Roscovitine. This would allow us to better study the actual recruitment of proteins at the fork without the limitation of pulling down more forks overall due to the action of CPT. In all, it is not possible to conclude that 100 nM CPT result in the increased presence of autophagy proteins based solely on our iPOND experiment.

Others also studied the role of autophagy in replication stress. For example, Vanzo and colleagues performed western blot analysis of whole cell extract in U2-OS cells after 2 hours of 100 nM and 1 μM CPT (Vanzo et al., 2020). They did not observe a change in LC3-B levels between untreated cells and cells that had been treated with these two doses of CPT. As we noticed an increased presence of LC3-B at the replication fork, this is an indication that 100 nM CPT could result in enhanced recruitment of this autophagy protein at the replication fork. More precisely, it could mean that the autophagy proteins are not upregulated overall upon treatment with nanomolar doses of CPT, but rather recruited to the nucleus where they are required. However, the active recruitment of autophagy proteins at sites of DNA damage after treatment with low-dose CPT still needs to be proven. More generally, Vanzo et al.'s study also provides additional evidence of the role of autophagy in resolving replication stress. They performed fiber assays in both MCF7 and HeLa cells and observed a reduction in fork progression speed in the absence of ATG5 and ATG7. Together these results suggest an important role for autophagy at the replication fork.

Autophagy Degrades Aggregated Proteins

One of the main roles of autophagy is the clearance of aggregated proteins, which can accumulate when misfolded proteins are not properly cleared (Simonsen and Wollert, 2022). We reasoned that nanomolar dose-induced TOP1cc could accumulate in aggregated form after treatment with CPT if not cleared by autophagy. Indeed, a large increase of aggregated proteins was seen in this condition (Figure 6). As expected, we also observed an increase of aggregated proteins in cells treated only with Bafilomycin: by inhibiting the acidification of lysosomes, we prevented some of the physiologic turnover of proteins. Furthermore, this could provide an explanation as to why the proteasome is irrelevant in the clearance of nanomolar dose-induced TOP1cc. In fact, the role of the proteasome in the degradation of TOP1cc has been extensively studied. Most of the studies have, however, been conducted with micromolar doses of CPT (Sun et al., 2021). Our findings suggest that nanomolar doses of CPT elicit a different type of DNA damage, which is sensed and degraded by a different pathway than that induced by micromolar doses.

In general, small and soluble proteins are degraded by the proteasome, whereas bulkier, insoluble proteins are preferentially degraded by autophagy (Ding and Yin, 2008). Some misfolded proteins that are soluble can still be degraded by the proteasome. However, bulky (> 2 μm) insoluble aggregates are degraded by autophagy (Lilienbaum, 2013). As TOP1 is a rather large protein with a molecular weight of 100kDa, it is unsurprising that autophagy is necessary for its degradation. A possible explanation as to why nanomolar dose-induced TOP1cc accumulate in aggregated form is the unfoldase p97. In fact, Fielden et al. have shown that the complex consisting of SPRTN, TEX264 and p97 is responsible for repairing TOP1cc caused by 100 nM CPT (Fielden et al., 2020). Misfolded proteins tend to expose hydrophobic fragments which cause them to self-aggregate (Moreno-Gonzalez and Soto, 2011). Thus, it is unsurprising that nanomolar dose-induced TOP1cc, that require unfolding by p97 for their repair, result in bulky aggregates degradable by autophagy. We hypothesise that nanomolar-dose induced TOP1cc aggregate and require autophagy for their degradation, which is not the case for micromolar dose-induced TOP1cc. Repeating this immunofluorescence assay with 1 μM CPT, which should not lead to the formation of aggregates if our hypothesis is correct. Additionally, performing this experiment again with synchronised cells should allow us to observe that the formation of aggregates only occurs in S phase cells, which should be experiencing nanomolar dose-induced replication stress.

To further confirm that the aggregates detected with the Proteostat dye were truly TOP1cc, we decided to transiently deplete TOP1 with siRNA (Figure 7). However, the depletion efficacy was quite low, and we were not able to see any difference in the formation of aggregates. Various attempts to improve the depletion efficacy were made. Firstly, we increased the amount of siRNA from 20ng to 40ng and used new Lipofectamine. Next, we depleted for 72 hours instead of 48. Finally, we lowered the seeding density to allow for a better uptake of the siRNA; however, no significant improvement was observed. An attempt was also made to biochemically purify the aggregated proteins but was unsuccessful.

Lamin A/C as a Marker for the Nuclear Envelope Plasticity after CPT Treatment

Lamin A/C localises at the periphery of the nucleus, between the nucleoplasm and the inner nuclear membrane (Dubik and Mai, 2020). As it has been described as a regulator of nuclear mechanics and stiffness (Lammerding et al., 2006), we decided to use it as a marker for the nuclear envelope (Figure 8). We were interested in studying the behavior of the nuclear envelope after treatment with CPT. We reasoned that CPT treatment would induce changes in the nuclear envelope that would allow the nuclear exit of TOP1cc and its subsequent incorporation into an autophagosome. However, we did not observe any significant differences in the nuclear shape after treatment with CPT. HeLa cells characteristically have abnormal nuclear shapes (Mishra and Levy, 2022). Since HeLa cells already have disrupted nuclear morphologies, attempting to notice additional abnormalities proved to be more complex than expected. Although it seems like CPT did not result in any changes to the nucleus shape, further experiments would have to be performed to accurately confirm this. We chose Lamin A/C also because it has a large portion of Lamin A, around 60%, which is mobile in the nucleoplasm (Naetar et al., 2017). We reasoned that its mobility could facilitate the study of its behavior after CPT treatment. Another limitation of our experiment is the fixation step. In fact, we fixed the cells after 1 hour of treatment with CPT. However, it is possible that the abnormality in lamina structure specific to CPT would occur just seconds after treatment with CPT or perhaps would require hours. Fixing at a specific time could result in the loss of the event we are interested in. It is also worth noting that the fixative agent used can have an impact on morphology of cells and cellular components (Paavilainen et al., 2010). In fact, a recent study observed Glyoxal to perform better than formaldehyde in fixation for immunohistochemistry studies of synapses (Konno et al., 2023). To tackle this issue, we generated a stable cell line, in which Lamin A/C was tagged with GFP. We used this cell line to perform live imaging before and after treatment with CPT. This allowed us to monitor Lamin A/C behavior overtime as well as avoid fixing with formaldehyde.

It is also possible that Lamin A/C was not the appropriate marker for this study. Another marker we could have used is Lamin B1. It is known that autophagic degradation of Lamin B1 is a marker of oncogene-induced senescence (Dou et al., 2015). In our case, which is independent of senescence, Lamin B1 could have been used, as it has very similar properties to Lamin A/C. It also localises as a circle around the nucleus next to the outer nuclear membrane and plays a role in maintenance of nuclear shape as well as regulation of gene expression (Shimi et al., 2011).

The reason for which we were interested in studying the behavior of the nuclear envelope was to better understand the mechanism by which TOP1cc exit the nucleus to be incorporated into the autophagosome. Another way to study the permeability of the nucleus could be to use a nuclear localisation signal. Nuclear localisation signals usually consist of short chains of amino acids that signal the import of proteins into the nucleus (Lu et al., 2021). Fusing mCherry to a nuclear localisation signal would allow us to visualise changes in nuclear permeability. For instance, if the nuclear envelope became ruptured after CPT treatment, this would result in the exit of the mCherry-fused nuclear localisation signal. However, nuclear trafficking is tightly regulated, and it is expected that mCherry would be transported back into the nucleus

due to its nuclear localisation signal. This represents a limitation of this type of experiment. However, other studies have used this technique and have not encountered this limitation (Vargas et al., 2012).

Lamin A/C Acetylation as Marker of Nuclear Envelope Permeability

Finally, we hypothesised that, perhaps, the nuclear envelope did not undergo specific morphological changes specific to treatment with CPT, but rather changes in its permeability. A study by Karoutas et al. showed that decreased levels of Lamin A/C acetylation resulted in higher levels of solubility and decreased maintenance of nuclear morphology (Karoutas et al., 2019). More precisely, they identified MOF as a lysine acetyltransferase whose target is Lamin A/C. They mutated the lysines on which the acetylation event occurred to arginine; they also generated MOF -/- stable cell lines. They performed electron microscopy and noticed that the nuclear lamina had a “fuzzy-like” structure. They also noted increased nuclear blebbing. Thus, we decided to study Lamin A/C acetylation (Figure 9). However, very variable results were observed, and no significant decrease of Lamin A/C acetylation were detected upon CPT exposure. To confirm that changes in Lamin A/C acetylation levels do not occur, studies of MOF levels could be performed. A general antibody against acetylated lysines was used, therefore confirmation with a further, more specific, experiment exploring MOF levels would be very useful. Furthermore, it would be very interesting to study the phosphorylation of Lamin A/C, as phosphorylation is what mediates its depolymerisation (Liu and Ikegami, 2020).

As no changes in both morphology of the nuclear envelope nor in acetylation levels of Lamin A/C were noted, we decided to perform volume electron microscopy to study the lipid bilayer of the nuclear envelope in detail. These experiments were performed both with chemical fixatives, which may alter morphology, and with fixation by freezing, to preserve all of the intracellular structures. They revealed that, upon treatment with CPT, a separation between the inner and outer nuclear membrane occurs, whereby the distance between these two layers increases significantly. A recent study by Kucińska et al. described a similar separation of the inner and outer nuclear membranes upon ER stress (Kucinska et al., 2023). Interestingly, they performed transmission electron microscopy experiments in which TEX264 was gold labelled and observed the presence of TEX264 in the space between the outer and inner nuclear membranes. It would be very interesting to perform the same experiment as Kucińska et al. but by labelling TOP1 with immunogold rather than TEX264. Taken together these findings hint that the nuclear envelope does undergo structural changes that allow the exit of TOP1cc.

TEX264 is SUMOylated after CPT Treatment

To study modifications of the TEX264 receptor, we first thought of ubiquitination (Figure 10), which is linked with protein degradation. Although ubiquitination has long been associated with the proteasome, ubiquitin also plays a key role in the positive regulation of autophagy (Chen et al., 2019). In ubiquitin-dependent autophagy, receptors bind ubiquitinated proteins selected for degradation. We performed several denaturing immunoprecipitation assays to study post-translational modifications and observed increased ubiquitination on TEX264 two times only. Ubiquitination of transmembrane proteins has been described as a mechanism for the regulation of their trafficking (Hicke and Dunn, 2003). Furthermore, it has been shown that ubiquitin also plays a role in regulating the availability of receptors to interact with their substrates (Huangfu and Fuchs, 2010). Although ubiquitination of TEX264 after treatment with CPT would have to be confirmed, it could signify a change in the availability of TEX264 to bind LC3 or a tag to select it and its substrates for autophagic degradation. More specifically, we have observed increased monoubiquitination of TEX264. Monoubiquitination is associated with protein sorting and trafficking (Ronai, 2016). This could suggest that the monoubiquitin on TEX264 could aid its localisation to the autophagosome.

Next, we studied SUMOylation events on TEX264 (Figure 10). SUMO has a large variety of functions, among which is the regulation of the DNA damage response, the regulation of gene expression and the maintenance of protein homeostasis (Vertegaal, 2022). TEX264 also has a SIM motif where it binds SUMOylated proteins (Fielden et al., 2020). However, we have shown that levels of SUMOylation on TEX264 itself increase after treatment with 50 nM CPT. Together, these facts indicate that TEX264 is both ubiquitinated and SUMOylated. It has been shown that SUMOylation can enhance autophagy to promote the clearance of protein aggregates (Vertegaal, 2022). More specifically a role for SUMOylation in the reduction of protein aggregation in diseases such as Alzheimer's Disease or Spinocerebellar Ataxin Type I has been described (Liebelt and Vertegaal, 2016). There is a large crosstalk between SUMO and ubiquitin. For instance, SUMO polymers can promote further ubiquitination of proteins, which will direct them to the proteasome for degradation (Vertegaal, 2022). More specifically, we observed mono-SUMOylation on TEX264. SUMO can also stabilise proteins by competing for the binding to selected lysines with ubiquitin, thus preventing their targeting for degradation. In our case, further experiments would have to be conducted to better understand the role of ubiquitination and SUMOylation on TEX264. First of all, it would be interesting to elucidate if these two events are independent from one another or if one has to happen for the other post-translational modification to occur. To explore this, the same denaturing experiment would have to be performed but with the inhibition of SUMO1 and then with the inhibition of ubiquitin. Additionally, it would be important to study if these modifications are essential for the incorporation of TOP1cc into the autophagosome. Performing a pull-down of lysosomes after inhibiting SUMO1 or ubiquitin could be a way to understand this. Mass spectrometry analysis could be used to find the lysine residues which are SUMOylated and ubiquitinated. Modification of these residues could be a more specific manner to approach the aforementioned questions.

TEX264 Mutants

In order to better study the role of TEX264 as a receptor for autophagy, various mutants of TEX264 were introduced into stable cell lines. As previously mentioned, TEX264 has a LIR, a SHP and TBS through which it binds LC3, p97 and TOP1. TEX264 with a mutation in each of these regions was reintroduced in TEX264 -/- cells. We performed various co-immunoprecipitation assays to confirm that the appropriate interactions were lost in each stable cell line (Figure 11). However, variable and unexpected results were observed. More specifically TOP1 mutant TEX264 did not lose interaction with TOP1. This is also true for the SHP mutant, which kept its interaction with p97. The LIR mutant, however, lost its interaction with both LC3 and p97. Furthermore, these results were not reproducible and changes in interactions kept and lost were observed. As these stable cell lines had different levels of TEX264 expression, various attempts had to be made to optimise the level of TEX264. To improve the results of the co-immunoprecipitation, various ideas were explored. For instance, we tried to transiently transfect additional LIR mutant TEX264 into the stable cell line to equilibrate TEX264 protein levels between the cell lines. We also tried to incubate all the cells with CPT to promote the interactions, as Fielden et al. showed that the complex of TEX264, TOP1 and p97 assembles for the repair of TOP1cc after treatment with CPT (Fielden et al., 2020). Finally, we reasoned that, perhaps, the stable cell lines had adapted to the mutations and decided to perform the co-immunoprecipitation after transient transfection of all the mutant versions of TEX264. As none of these ideas proved to be the solution, we then decided to use HeLa cells as controls and study each stable cell line separately. This was done to avoid having to use each stable cell line as a control for the others.

Future Directions

First of all, it would be interesting to further explore the different type of DNA damage caused by nanomolar and micromolar doses of CPT. Performing a COMET assay with cells treated with both doses would be a potential way to further confirm that micromolar doses of CPT cause double-strand breaks. We believe that autophagy resolves the DNA damage caused by nanomolar doses of CPT, which is replication stress. Autophagy, however, does not play a role in the repair of double-strand breaks caused by micromolar doses of CPT. A DNA fiber assay allows us to monitor the speed of fork progression. Using cells with an ATG7 depletion, it would be interesting to perform a fiber assay after treatment with both 50 nM CPT and 1 μM CPT. If our hypothesis is correct, the depletion of ATG7 to prevent selective autophagy should further decrease fork progression only in cells treated with 50 nM CPT. However, the cells treated with 1μM CPT should not be affected in their fork progression by this depletion. Torin is a potent booster of the autophagy pathway (Kim and Guan, 2015). Using Torin in these conditions should increase the speed of fork progression in cells treated with 50 nM CPT but not cells treated with 1 μM CPT.

Another important factor that we need to further elucidate is the post-translational modifications on TEX264. First it is necessary to clarify if one of these modifications depends on the other. Inhibiting SUMO1 or ubiquitin and performing a denaturing immunoprecipitation is one way to attempt this. For instance, if SUMOylation depends on ubiquitination, inhibiting ubiquitin would prevent the SUMOylation event and vice versa. Mass spectrometry can be used to detect which lysines of TEX264 are SUMOylated and ubiquitinated. After discovering which lysines are modified, we could mutate them to prevent the ubiquitination and SUMOylation from occurring. Next, we could assess whether these modifications are essential for the autophagic degradation of TOP1cc mediated by TEX264. Finally, it is necessary to uncover the E3 ligases responsible for these modifications.

Ultimately, it would be worth gaining better mechanistic insight into the separation of inner and outer nuclear membranes after CPT treatment. The study by Kucińska et al. shows that the space between the inner and outer nuclear membranes is due to the reduction of the disulfide bond between SUN proteins and NESPRINs (Kucinska et al., 2023). In essence these proteins play a key role in maintaining the two layers of the nuclear envelope close together. They discovered that the reductase responsible for the break of the bond is TMX4. Additionally, they identified Zdhhc6 as a driver of palmitoylation-mediated regulation of TMX4. This could be a potential mechanism by which the two lipid bilayers separate upon treatment with CPT. To test this hypothesis, we could deplete TMX4 and observe whether the separation of inner and outer nuclear membrane still occurs.

Conclusions

It has been extensively described that micromolar doses of CPT cause double-strand breaks. The resulting TOP1cc are degraded by the proteasome. First, we distinguished the type of DNA damage caused by nanomolar doses of CPT from that caused by micromolar doses of CPT. We found that 50 nM CPT resulted in replication stress and not double-strand breaks. As TEX264 is an autophagy receptor, we hypothesised that autophagy could play a role in the degradation of TOP1cc. Our iPOND data alone did not allow us to make conclusions on the recruitment of autophagy proteins at the replication fork after 100 nM CPT. However, taken together with Nakamura et al. and Vanzo et al.'s data, it does seem like low-dose CPT calls the autophagy machinery into play. We then proceeded to find the reason for which different degradation pathways are needed for these two doses of CPT. In fact, after 100 nM CPT, p97 unfolds the TOP1cc. This causes the protein to accumulate in aggregated form, hard to process by the proteasome. However, we unsuccessfully attempted to deplete TOP1 to confirm it was the aggregated protein. We subsequently uncovered that the autophagy receptor TEX264 is both ubiquitinated and SUMOylated. More experiments would have to be performed to better understand the relevance of these modifications as well as the E3 ligases involved. Finally, we studied the nuclear envelope and its behavior upon treatment with CPT. We first attempted to use Lamin A/C as a nuclear envelope marker. However, we observed no significant differences in nuclear morphology after treatment with CPT. Thus, we decided to focus on Lamin A/C modifications that could alter its permeability after treatment. As decreased acetylation of Lamin A/C has been shown to increase its solubility, we reasoned that it could be the mechanism by which TOP1cc exits the nucleus. Nevertheless, Lamin A/C acetylation levels were unchanged after CPT treatment. Other candidate proteins, such as TMX4, are worth investigating for the better understanding of this exit mechanism. Various other experiments would have to be performed for the complete comprehension of the autophagic degradation of TOP1cc. In all, we have shown that autophagy plays a key role in the degradation of TOP1cc induced by nanomolar doses of CPT.

Model

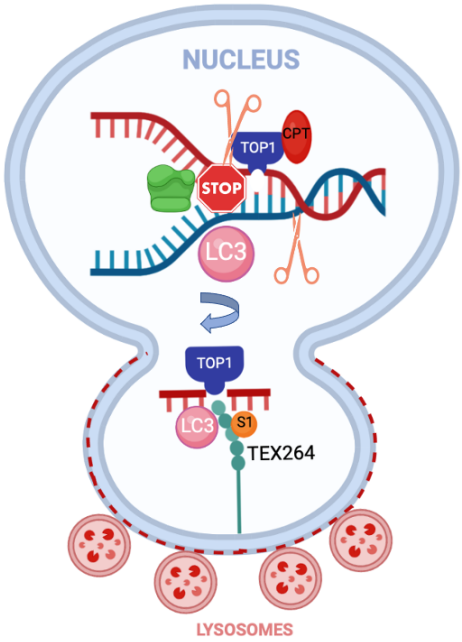


Figure 12. Model of Autophagic Degradation of TOP1cc. Nanomolar doses of CPT cause TOP1cc and replication stress. The autophagy machinery is recruited at the stalled replication fork and clear out proteotoxic aggregates. The receptor for this pathway is TEX264, which is SUMOylated upon treatment with CPT. The nuclear lamina does not undergo any changes in morphology or permeability. We believe that the separation between inner and outer nuclear membranes occurs to allow the incorporation of TOP1 into the autophagosome. Created with BioRender.

Acknowledgments

I would like to thank Prof. Kristijan Ramadan for allowing me to join his group and for his constant help and supervision. I am grateful to the entire Ramadan lab for their support and advice. A special thanks to Dr. Pauline Lascaux who has been my day-to-day supervisor. She has taught me numerous techniques and has helped me develop my scientific thinking and improve my experimental design. I am grateful for her continuous moral and academic support.

Reference List

AGROTIS, A. & KETTELER, R. 2019. On ATG4B as Drug Target for Treatment of Solid Tumours-The Knowns and the Unknowns. *Cells,* 9.

AMBROSIO, S. & MAJELLO, B. 2020. Autophagy Roles in Genome Maintenance. *Cancers (Basel),* 12.

AN, H., ORDUREAU, A., PAULO, J. A., SHOEMAKER, C. J., DENIC, V. & HARPER, J. W. 2019. TEX264 Is an Endoplasmic Reticulum-Resident ATG8-Interacting Protein Critical for ER Remodeling during Nutrient Stress. *Mol Cell,* 74, 891-908 e10.

AWASTHI, P., FOIANI, M. & KUMAR, A. 2015. ATM and ATR signaling at a glance. *J Cell Sci,* 128, 4255-62.

BAGNOLI, S., TERZIBASI TOZZINI, E. & CELLERINO, A. 2023. Immunofluorescence and Aggresome Staining of Nothobranchius furzeri Cryosections. *Cold Spring Harb Protoc*.

BASU, A. K. 2018. DNA Damage, Mutagenesis and Cancer. *Int J Mol Sci,* 19.

BO OTTO, F. & THUMM, M. 2020. Nucleophagy-Implications for Microautophagy and Health. *Int J Mol Sci,* 21.

BOUSSET, K. & DIFFLEY, J. F. 1998. The Cdc7 protein kinase is required for origin firing during S phase. *Genes Dev,* 12, 480-90.

BURNHAM, D. R., KOSE, H. B., HOYLE, R. B. & YARDIMCI, H. 2019. The mechanism of DNA unwinding by the eukaryotic replicative helicase. *Nat Commun,* 10, 2159.

CHANG, H. H. Y., PANNUNZIO, N. R., ADACHI, N. & LIEBER, M. R. 2017. Non-homologous DNA end joining and alternative pathways to double-strand break repair. *Nat Rev Mol Cell Biol,* 18, 495-506.

CHEN, R. H., CHEN, Y. H. & HUANG, T. Y. 2019. Ubiquitin-mediated regulation of autophagy. *J Biomed Sci,* 26, 80.

CHINO, H., HATTA, T., NATSUME, T. & MIZUSHIMA, N. 2019. Intrinsically Disordered Protein TEX264 Mediates ER-phagy. *Mol Cell,* 74, 909-921 e6.

CHOWDHURI, S. P. & DAS, B. B. 2021. Top1-PARP1 association and beyond: from DNA topology to break repair. *NAR Cancer,* 3, zcab003.

DAS, G., SHRAVAGE, B. V. & BAEHRECKE, E. H. 2012. Regulation and function of autophagy during cell survival and cell death. *Cold Spring Harb Perspect Biol,* 4.

DESAI, S. D., LI, T. K., RODRIGUEZ-BAUMAN, A., RUBIN, E. H. & LIU, L. F. 2001. Ubiquitin/26S proteasome-mediated degradation of topoisomerase I as a resistance mechanism to camptothecin in tumor cells. *Cancer Res,* 61, 5926-32.

DING, W. X. & YIN, X. M. 2008. Sorting, recognition and activation of the misfolded protein degradation pathways through macroautophagy and the proteasome. *Autophagy,* 4, 141-50.

DOU, Z., XU, C., DONAHUE, G., SHIMI, T., PAN, J. A., ZHU, J., IVANOV, A., CAPELL, B. C., DRAKE, A. M., SHAH, P. P., CATANZARO, J. M., RICKETTS, M. D., LAMARK, T., ADAM, S. A., MARMORSTEIN, R., ZONG, W. X., JOHANSEN, T., GOLDMAN, R. D., ADAMS, P. D. & BERGER, S. L. 2015. Autophagy mediates degradation of nuclear lamina. *Nature,* 527, 105-9.

DUBIK, N. & MAI, S. 2020. Lamin A/C: Function in Normal and Tumor Cells. *Cancers (Basel),* 12.

DUNGRAWALA, H. & CORTEZ, D. 2015. Purification of proteins on newly synthesized DNA using iPOND. *Methods Mol Biol,* 1228, 123-31.

FIELDEN, J., POPOVIC, M. & RAMADAN, K. 2022. TEX264 at the intersection of autophagy and DNA repair. *Autophagy,* 18, 40-49.

FIELDEN, J., WISEMAN, K., TORRECILLA, I., LI, S., HUME, S., CHIANG, S. C., RUGGIANO, A., NARAYAN SINGH, A., FREIRE, R., HASSANIEH, S., DOMINGO, E., VENDRELL, I., FISCHER, R., KESSLER, B. M., MAUGHAN, T. S., EL-KHAMISY, S. F. & RAMADAN, K. 2020. TEX264 coordinates p97- and SPRTN-mediated resolution of topoisomerase 1-DNA adducts. *Nat Commun,* 11, 1274.

FISHER, D. Z., CHAUDHARY, N. & BLOBEL, G. 1986. cDNA sequencing of nuclear lamins A and C reveals primary and secondary structural homology to intermediate filament proteins. *Proc Natl Acad Sci U S A,* 83, 6450-4.

FUJITA, K., KUBOTA, Y., ISHIDA, H. & SASAKI, Y. 2015. Irinotecan, a key chemotherapeutic drug for metastatic colorectal cancer. *World J Gastroenterol,* 21, 12234-48.

GAGOU, M. E., ZUAZUA-VILLAR, P. & MEUTH, M. 2010. Enhanced H2AX phosphorylation, DNA replication fork arrest, and cell death in the absence of Chk1. *Mol Biol Cell,* 21, 739-52.

GAILLARD, H., GARCIA-MUSE, T. & AGUILERA, A. 2015. Replication stress and cancer. *Nat Rev Cancer,* 15, 276-89.
GMEINER, W. H. 2019. Entrapment of DNA topoisomerase-DNA complexes by nucleotide/nucleoside analogs. *Cancer Drug Resist,* 2, 994-1001.
GUO, H. J., RAHIMI, N. & TADI, P. 2023. Biochemistry, Ubiquitination. *StatPearls.* Treasure Island (FL).
GUPTA, A., HUNT, C. R., CHAKRABORTY, S., PANDITA, R. K., YORDY, J., RAMNARAIN, D. B., HORIKOSHI, N. & PANDITA, T. K. 2014. Role of 53BP1 in the regulation of DNA double-strand break repair pathway choice. *Radiat Res,* 181, 1-8.
HANAHAN, D. 2022. Hallmarks of Cancer: New Dimensions. *Cancer Discov,* 12, 31-46.
HETZER, M. W. 2010. The nuclear envelope. *Cold Spring Harb Perspect Biol,* 2, a000539.
HEWITT, G. & KOROLCHUK, V. I. 2017. Repair, Reuse, Recycle: The Expanding Role of Autophagy in Genome Maintenance. *Trends Cell Biol,* 27, 340-351.
HICKE, L. & DUNN, R. 2003. Regulation of membrane protein transport by ubiquitin and ubiquitin-binding proteins. *Annu Rev Cell Dev Biol,* 19, 141-72.
HOLDGAARD, S. G., CIANFANELLI, V., PUPO, E., LAMBRUGHI, M., LUBAS, M., NIELSEN, J. C., EIBES, S., MAIANI, E., HARDER, L. M., WESCH, N., FOGED, M. M., MAEDA, K., NAZIO, F., DE LA BALLINA, L. R., DOTSCH, V., BRECH, A., FRANKEL, L. B., JAATTELA, M., LOCATELLI, F., BARISIC, M., ANDERSEN, J. S., BEKKER-JENSEN, S., LUND, A. H., ROGOV, V. V., PAPALEO, E., LANZETTI, L., DE ZIO, D. & CECCONI, F. 2019. Selective autophagy maintains centrosome integrity and accurate mitosis by turnover of centriolar satellites. *Nat Commun,* 10, 4176.
HUANG, T. H., CHEN, H. C., CHOU, S. M., YANG, Y. C., FAN, J. R. & LI, T. K. 2010. Cellular processing determinants for the activation of damage signals in response to topoisomerase I-linked DNA breakage. *Cell Res,* 20, 1060-75.
HUANGFU, W. C. & FUCHS, S. Y. 2010. Ubiquitination-dependent regulation of signaling receptors in cancer. *Genes Cancer,* 1, 725-34.
IANNASCOLI, C., PALERMO, V., MURFUNI, I., FRANCHITTO, A. & PICHIERRI, P. 2015. The WRN exonuclease domain protects nascent strands from pathological MRE11/EXO1-dependent degradation. *Nucleic Acids Res,* 43, 9788-803.
JOHANSEN, T. & LAMARK, T. 2011. Selective autophagy mediated by autophagic adapter proteins. *Autophagy,* 7, 279-96.
KANG, R., ZEH, H. J., LOTZE, M. T. & TANG, D. 2011. The Beclin 1 network regulates autophagy and apoptosis. *Cell Death Differ,* 18, 571-80.
KARANTZA-WADSWORTH, V., PATEL, S., KRAVCHUK, O., CHEN, G., MATHEW, R., JIN, S. & WHITE, E. 2007. Autophagy mitigates metabolic stress and genome damage in mammary tumorigenesis. *Genes Dev,* 21, 1621-35.
KAROUTAS, A. & AKHTAR, A. 2021. Functional mechanisms and abnormalities of the nuclear lamina. *Nat Cell Biol,* 23, 116-126.
KAROUTAS, A., SZYMANSKI, W., RAUSCH, T., GUHATHAKURTA, S., ROG-ZIELINSKA, E. A., PEYRONNET, R., SEYFFERTH, J., CHEN, H. R., DE LEEUW, R., HERQUEL, B., KIMURA, H., MITTLER, G., KOHL, P., MEDALIA, O., KORBEL, J. O. & AKHTAR, A. 2019. The NSL complex maintains nuclear architecture stability via lamin A/C acetylation. *Nat Cell Biol,* 21, 1248-1260.
KATYAL, S., LEE, Y., NITISS, K. C., DOWNING, S. M., LI, Y., SHIMADA, M., ZHAO, J., RUSSELL, H. R., PETRINI, J. H., NITISS, J. L. & MCKINNON, P. J. 2014. Aberrant topoisomerase-1 DNA lesions are pathogenic in neurodegenerative genome instability syndromes. *Nat Neurosci,* 17, 813-21.
KELMAN, Z. 1997. PCNA: structure, functions and interactions. *Oncogene,* 14, 629-40.
KILGAS, S., SINGH, A. N., PAILLAS, S., THEN, C. K., TORRECILLA, I., NICHOLSON, J., BROWNING, L., VENDRELL, I., KONIETZNY, R., KESSLER, B. M., KILTIE, A. E. & RAMADAN, K. 2021. p97/VCP inhibition causes excessive MRE11-dependent DNA end resection promoting cell killing after ionizing radiation. *Cell Rep,* 35, 109153.
KIM, Y. C. & GUAN, K. L. 2015. mTOR: a pharmacologic target for autophagy regulation. *J Clin Invest,* 125, 25-32.
KOCH, A. J. & HOLASKA, J. M. 2014. Emerin in health and disease. *Semin Cell Dev Biol,* 29, 95-106.
KONNO, K., YAMASAKI, M., MIYAZAKI, T. & WATANABE, M. 2023. Glyoxal fixation: An approach to solve immunohistochemical problem in neuroscience research. *Sci Adv,* 9, eadf7084.
KRASTEV, D. B., LI, S., SUN, Y., WICKS, A. J., HOSLETT, G., WEEKES, D., BADDER, L. M., KNIGHT, E. G., MARLOW, R., PARDO, M. C., YU, L., TALELE, T. T., BARTEK, J., CHOUDHARY, J. S.,

POMMIER, Y., PETTITT, S. J., TUTT, A. N. J., RAMADAN, K. & LORD, C. J. 2022. The ubiquitin-dependent ATPase p97 removes cytotoxic trapped PARP1 from chromatin. *Nat Cell Biol,* 24, 62-73.
KUCINSKA, M. K., FEDRY, J., GALLI, C., MORONE, D., RAIMONDI, A., SOLDA, T., FORSTER, F. & MOLINARI, M. 2023. TMX4-driven LINC complex disassembly and asymmetric autophagy of the nuclear envelope upon acute ER stress. *Nat Commun,* 14, 3497.
KUMAR, A., MAZZANTI, M., MISTRIK, M., KOSAR, M., BEZNOUSSENKO, G. V., MIRONOV, A. A., GARRE, M., PARAZZOLI, D., SHIVASHANKAR, G. V., SCITA, G., BARTEK, J. & FOIANI, M. 2014. ATR mediates a checkpoint at the nuclear envelope in response to mechanical stress. *Cell,* 158, 633-46.
LAMARK, T. & JOHANSEN, T. 2012. Aggrephagy: selective disposal of protein aggregates by macroautophagy. *Int J Cell Biol,* 2012, 736905.
LAMMERDING, J., FONG, L. G., JI, J. Y., REUE, K., STEWART, C. L., YOUNG, S. G. & LEE, R. T. 2006. Lamins A and C but not lamin B1 regulate nuclear mechanics. *J Biol Chem,* 281, 25768-80.
LEE, E. Y. & MULLER, W. J. 2010. Oncogenes and tumor suppressor genes. *Cold Spring Harb Perspect Biol,* 2, a003236.
LEE, Y. K. & LEE, J. A. 2016. Role of the mammalian ATG8/LC3 family in autophagy: differential and compensatory roles in the spatiotemporal regulation of autophagy. *BMB Rep,* 49, 424-30.
LI, X. & HEYER, W. D. 2008. Homologous recombination in DNA repair and DNA damage tolerance. *Cell Res,* 18, 99-113.
LIEBELT, F. & VERTEGAAL, A. C. 2016. Ubiquitin-dependent and independent roles of SUMO in proteostasis. *Am J Physiol Cell Physiol,* 311, C284-96.
LILIENBAUM, A. 2013. Relationship between the proteasomal system and autophagy. *Int J Biochem Mol Biol,* 4, 1-26.
LINDAHL, T. 1993. Instability and decay of the primary structure of DNA. *Nature,* 362, 709-15.
LIU, L. F. & WANG, J. C. 1987. Supercoiling of the DNA template during transcription. *Proc Natl Acad Sci U S A,* 84, 7024-7.
LIU, S. Y. & IKEGAMI, K. 2020. Nuclear lamin phosphorylation: an emerging role in gene regulation and pathogenesis of laminopathies. *Nucleus,* 11, 299-314.
LU, J., WU, T., ZHANG, B., LIU, S., SONG, W., QIAO, J. & RUAN, H. 2021. Types of nuclear localization signals and mechanisms of protein import into the nucleus. *Cell Commun Signal,* 19, 60.
MARTIN, L. J. 2008. DNA damage and repair: relevance to mechanisms of neurodegeneration. *J Neuropathol Exp Neurol,* 67, 377-87.
MISHRA, S. & LEVY, D. L. 2022. Nuclear F-actin and Lamin A antagonistically modulate nuclear shape. *J Cell Sci,* 135.
MORENO-GONZALEZ, I. & SOTO, C. 2011. Misfolded protein aggregates: mechanisms, structures and potential for disease transmission. *Semin Cell Dev Biol,* 22, 482-7.
MUZI-FALCONI, M., GIANNATTASIO, M., FOIANI, M. & PLEVANI, P. 2003. The DNA polymerase alpha-primase complex: multiple functions and interactions. *ScientificWorldJournal,* 3, 21-33.
MYLONAS, A. & O'LOGHLEN, A. 2022. Cellular Senescence and Ageing: Mechanisms and Interventions. *Front Aging,* 3, 866718.
NAETAR, N., FERRAIOLI, S. & FOISNER, R. 2017. Lamins in the nuclear interior - life outside the lamina. *J Cell Sci,* 130, 2087-2096.
NAKAMURA, K., KUSTATSCHER, G., ALABERT, C., HODL, M., FORNE, I., VOLKER-ALBERT, M., SATPATHY, S., BEYER, T. E., MAILAND, N., CHOUDHARY, C., IMHOF, A., RAPPSILBER, J. & GROTH, A. 2021. Proteome dynamics at broken replication forks reveal a distinct ATM-directed repair response suppressing DNA double-strand break ubiquitination. *Mol Cell,* 81, 1084-1099 e6.
NAKATOGAWA, H. 2013. Two ubiquitin-like conjugation systems that mediate membrane formation during autophagy. *Essays Biochem,* 55, 39-50.
PAAVILAINEN, L., EDVINSSON, A., ASPLUND, A., HOBER, S., KAMPF, C., PONTEN, F. & WESTER, K. 2010. The impact of tissue fixatives on morphology and antibody-based protein profiling in tissues and cells. *J Histochem Cytochem,* 58, 237-46.
PANDE, S. & GHOSH, D. K. 2023. Nuclear proteostasis imbalance in laminopathy-associated premature aging diseases. *FASEB J,* 37, e23116.

PARK, S. S., EOM, Y. W. & CHOI, K. S. 2005. Cdc2 and Cdk2 play critical roles in low dose doxorubicin-induced cell death through mitotic catastrophe but not in high dose doxorubicin-induced apoptosis. *Biochem Biophys Res Commun,* 334, 1014-21.

POMMIER, Y., BARCELO, J. M., RAO, V. A., SORDET, O., JOBSON, A. G., THIBAUT, L., MIAO, Z. H., SEILER, J. A., ZHANG, H., MARCHAND, C., AGAMA, K., NITISS, J. L. & REDON, C. 2006. Repair of topoisomerase I-mediated DNA damage. *Prog Nucleic Acid Res Mol Biol,* 81, 179-229.

POMMIER, Y., NUSSENZWEIG, A., TAKEDA, S. & AUSTIN, C. 2022. Human topoisomerases and their roles in genome stability and organization. *Nat Rev Mol Cell Biol,* 23, 407-427.

PRAKASH, R., ZHANG, Y., FENG, W. & JASIN, M. 2015. Homologous recombination and human health: the roles of BRCA1, BRCA2, and associated proteins. *Cold Spring Harb Perspect Biol,* 7, a016600.

RAMADAN, K., HALDER, S., WISEMAN, K. & VAZ, B. 2017. Strategic role of the ubiquitin-dependent segregase p97 (VCP or Cdc48) in DNA replication. *Chromosoma,* 126, 17-32.

RAY CHAUDHURI, A., HASHIMOTO, Y., HERRADOR, R., NEELSEN, K. J., FACHINETTI, D., BERMEJO, R., COCITO, A., COSTANZO, V. & LOPES, M. 2012. Topoisomerase I poisoning results in PARP-mediated replication fork reversal. *Nat Struct Mol Biol,* 19, 417-23.

RIBEYRE, C., ZELLWEGER, R., CHAUVIN, M., BEC, N., LARROQUE, C., LOPES, M. & CONSTANTINOU, A. 2016. Nascent DNA Proteomics Reveals a Chromatin Remodeler Required for Topoisomerase I Loading at Replication Forks. *Cell Rep,* 15, 300-9.

RONAI, Z. A. 2016. Monoubiquitination in proteasomal degradation. *Proc Natl Acad Sci U S A,* 113, 8894-6.

SATOO, K., NODA, N. N., KUMETA, H., FUJIOKA, Y., MIZUSHIMA, N., OHSUMI, Y. & INAGAKI, F. 2009. The structure of Atg4B-LC3 complex reveals the mechanism of LC3 processing and delipidation during autophagy. *EMBO J,* 28, 1341-50.

SCHOONEN, P. M., GUERRERO LLOBET, S. & VAN VUGT, M. 2019. Replication stress: Driver and therapeutic target in genomically instable cancers. *Adv Protein Chem Struct Biol,* 115, 157-201.

SHI, X., YOKOM, A. L., WANG, C., YOUNG, L. N., YOULE, R. J. & HURLEY, J. H. 2020. ULK complex organization in autophagy by a C-shaped FIP200 N-terminal domain dimer. *J Cell Biol,* 219.

SHIMI, T., BUTIN-ISRAELI, V., ADAM, S. A., HAMANAKA, R. B., GOLDMAN, A. E., LUCAS, C. A., SHUMAKER, D. K., KOSAK, S. T., CHANDEL, N. S. & GOLDMAN, R. D. 2011. The role of nuclear lamin B1 in cell proliferation and senescence. *Genes Dev,* 25, 2579-93.

SIMONSEN, A. & WOLLERT, T. 2022. Don't forget to be picky - selective autophagy of protein aggregates in neurodegenerative diseases. *Curr Opin Cell Biol,* 75, 102064.

SIRBU, B. M., COUCH, F. B. & CORTEZ, D. 2012. Monitoring the spatiotemporal dynamics of proteins at replication forks and in assembled chromatin using isolation of proteins on nascent DNA. *Nat Protoc,* 7, 594-605.

SLICHENMYER, W. J., ROWINSKY, E. K., DONEHOWER, R. C. & KAUFMANN, S. H. 1993. The current status of camptothecin analogues as antitumor agents. *J Natl Cancer Inst,* 85, 271-91.

STINGELE, J., BELLELLI, R., ALTE, F., HEWITT, G., SAREK, G., MASLEN, S. L., TSUTAKAWA, S. E., BORG, A., KJAER, S., TAINER, J. A., SKEHEL, J. M., GROLL, M. & BOULTON, S. J. 2016. Mechanism and Regulation of DNA-Protein Crosslink Repair by the DNA-Dependent Metalloprotease SPRTN. *Mol Cell,* 64, 688-703.

SUN, Y., CHEN, J., HUANG, S. N., SU, Y. P., WANG, W., AGAMA, K., SAHA, S., JENKINS, L. M., PASCAL, J. M. & POMMIER, Y. 2021. PARylation prevents the proteasomal degradation of topoisomerase I DNA-protein crosslinks and induces their deubiquitylation. *Nat Commun,* 12, 5010.

SUN, Y., SAHA, L. K., SAHA, S., JO, U. & POMMIER, Y. 2020. Debulking of topoisomerase DNA-protein crosslinks (TOP-DPC) by the proteasome, non-proteasomal and non-proteolytic pathways. *DNA Repair (Amst),* 94, 102926.

TAKAHASHI, Y., HE, H., TANG, Z., HATTORI, T., LIU, Y., YOUNG, M. M., SERFASS, J. M., CHEN, L., GEBRU, M., CHEN, C., WILLS, C. A., ATKINSON, J. M., CHEN, H., ABRAHAM, T. & WANG, H. G. 2018. An autophagy assay reveals the ESCRT-III component CHMP2A as a regulator of phagophore closure. *Nat Commun,* 9, 2855.

TAKIMOTO, C. H. & ARBUCK, S. G. 1997. Clinical status and optimal use of topotecan. *Oncology (Williston Park),* 11, 1635-46; discussion 1649-51, 1655-7.

TIAN, X., TENG, J. & CHEN, J. 2021. New insights regarding SNARE proteins in autophagosome-lysosome fusion. *Autophagy,* 17, 2680-2688.
VANZO, R., BARTKOVA, J., MERCHUT-MAYA, J. M., HALL, A., BOUCHAL, J., DYRSKJOT, L., FRANKEL, L. B., GORGOULIS, V., MAYA-MENDOZA, A., JAATTELA, M. & BARTEK, J. 2020. Autophagy role(s) in response to oncogenes and DNA replication stress. *Cell Death Differ,* 27, 1134-1153.
VARGAS, J. D., HATCH, E. M., ANDERSON, D. J. & HETZER, M. W. 2012. Transient nuclear envelope rupturing during interphase in human cancer cells. *Nucleus,* 3, 88-100.
VAZ, B., POPOVIC, M., NEWMAN, J. A., FIELDEN, J., AITKENHEAD, H., HALDER, S., SINGH, A. N., VENDRELL, I., FISCHER, R., TORRECILLA, I., DROBNITZKY, N., FREIRE, R., AMOR, D. J., LOCKHART, P. J., KESSLER, B. M., MCKENNA, G. W., GILEADI, O. & RAMADAN, K. 2016. Metalloprotease SPRTN/DVC1 Orchestrates Replication-Coupled DNA-Protein Crosslink Repair. *Mol Cell,* 64, 704-719.
VERTEGAAL, A. C. O. 2022. Signalling mechanisms and cellular functions of SUMO. *Nat Rev Mol Cell Biol,* 23, 715-731.
WANG, J. C. 2002. Cellular roles of DNA topoisomerases: a molecular perspective. *Nat Rev Mol Cell Biol,* 3, 430-40.
WATSON, M. L. 1955. The nuclear envelope; its structure and relation to cytoplasmic membranes. *J Biophys Biochem Cytol,* 1, 257-70.
WEICKERT, P. & STINGELE, J. 2022. DNA-Protein Crosslinks and Their Resolution. *Annu Rev Biochem,* 91, 157-181.
WOODS, D. & TURCHI, J. J. 2013. Chemotherapy induced DNA damage response: convergence of drugs and pathways. *Cancer Biol Ther,* 14, 379-89.
XU, Y., WU, X. & HER, C. 2015. hMSH5 Facilitates the Repair of Camptothecin-induced Double-strand Breaks through an Interaction with FANCJ. *J Biol Chem,* 290, 18545-58.
YANG, S. W., BURGIN, A. B., JR., HUIZENGA, B. N., ROBERTSON, C. A., YAO, K. C. & NASH, H. A. 1996. A eukaryotic enzyme that can disjoin dead-end covalent complexes between DNA and type I topoisomerases. *Proc Natl Acad Sci U S A,* 93, 11534-9.
YU, L., CHEN, Y. & TOOZE, S. A. 2018. Autophagy pathway: Cellular and molecular mechanisms. *Autophagy,* 14, 207-215.
ZAFFAGNINI, G. & MARTENS, S. 2016. Mechanisms of Selective Autophagy. *J Mol Biol,* 428, 1714-24.
ZHANG, H., XIONG, Y. & CHEN, J. 2020. DNA-protein cross-link repair: what do we know now? *Cell Biosci,* 10, 3.